Flexible Thermo-Camouflage materials in Supersonic Flowfields with Selective Energy Dissipation

Namkyu Lee[a,b], Joon-Soo Lim[b], Injoong Chang[b], Donghwi Lee[c], Hyung Hee Cho[b,*]

a. IBI-4, Forschungszentrum Jülich GmbH, 52425 Jülich, Germany

b. Department of Mechanical Engineering, Yonsei University, 50 Yonsei-ro, Seodaemun-gu, Seoul 13722, Korea

c. Department of Mechanical Engineering, University of Wisconsin–Madison, 1500 Engineering Drive, Madison, WI 53706, United States

* Corresponding author

Tel.: +82 2 2123 2828

Fax: +82 2 312 2159

E-mail: hhcho@yonsei.ac.kr

Abstract

Camouflage refers to a creature's behavior to protect itself from predators by assimilating its signature with the environment. In particular, thermal camouflage materials in infrared (IR) wave are attracting interest for energy, military and space applications. To date, several types of camouflage materials such as photonic crystals and metal-dielectric-metal structures have been developed. However, flexible camouflage materials are still challenging issues because of the material's brittleness and anomalous dispersion. Herein, we propose flexible thermo-camouflage materials (FTCM) for IR camouflage on an arbitrary surface without mechanical failure. Without using a polymer as a dielectric layer, we realized FTCM by changing the unit cell structure discretely. Through imaging methods, we verified their flexibility, machinability and IR camouflage performance. We also measured and calculated the spectral emissivity of FTCM; they showed electromagnetic behavior similar to a conventional emitter. We quantified the IR camouflage performance of FTCM that the emissivity in the undetected band (5–8 μm) is 0.27, and the emissivity in detected bands are 0.12 (3–5 μm) and 0.16 (8–14 μm) in the detected bands, respectively. Finally, we confirmed the IR camouflage performance on an arbitrary surface in a supersonic flowfield. FTCM are expected to help improving our basic understanding of metamaterials and find widespread application as IR camouflage materials.

Keywords:

Flexible camouflage materials; Thermal camouflage; IR camouflage; Energy dissipation; Selective emitter;

1. Introduction

Camouflage means a creature's ability to hide itself from external threats by blending in with its environment and well-known examples of such creatures are chameleons and cephalopods[1,2]. Artificial camouflage materials capable of changing their signature have attracted research interest for use in displays[3] and bio-inspired structures[4,5]. The field thermal camouflage materials, infrared (IR) wave ranging the spectrum from 0.7 μm to 1000 μm, has become an emerging field of research owing to the potential of these materials for energy conversion[6,7], radiative cooling[8–10], and space applications[11]. Therefore, many researchers have investigated IR camouflage materials to control their electromagnetic (EM) behavior in line with intended applications[12,13].

To control the IR signature from the surface, either the temperature or the emissivity are manipulated by external materials based on the Stefan-Boltzmann law, $q'' = \varepsilon\sigma T^4$ (ε: emissivity, σ: Stefan-Boltzmann constant and T: Temperature)[14]. In order to control the IR signature from the targets, the temperature[15,16] and emissivity[17–22] can be controlled by the IR camouflage materials. In case of the emissivity-controlled materials, they do not need no additional devices and larger controlling range of IR signature[17–23]. For IR camouflage materials, controlling the emissivity need two requirements: decrease their IR signature in the detected band and increase energy dissipation of reduced IR signature in the undetected band for preventing the thermal instability[24]. By considering atmospheric transmittance[25], the IR detection wavelength ranges 3–5 μm and 8–14 μm are called the detected bands and IR waves in the wavelength range 5–8 μm are termed the undetected band which are absorbed by water and carbon dioxide in the air. In IR camouflage materials utilizing these characteristics, the target signature is reduced in the detected bands. Moreover, the reduced IR signature causing thermal instability should be dissipated in the undetected band based on the energy conservation. Several researchers have developed IR camouflage materials satisfying these requirements and demonstrated IR camouflage performance by using an IR camera[18,20,26].

Present research is focused on enhancing the flexibility of IR camouflage materials while maintaining their performance, since most surfaces in the real world are curved[27–29]. However, achieving flexibility and high performance simultaneously is difficult, owing to the limitation of the materials. Typically, IR camouflage materials have a metal-dielectric-metal (MDM) structure. For the dielectric layer, the ceramic materials such as zinc sulfide[17], alumina[30] and silicon nitride[31] are used. The problem with ceramic materials is that they are too brittle and hence cannot be bent by applying an external force. Even if their thickness is reduced to the order of 10 nm, a 1% change in their structure leads to fracture[32]. Replacing the dielectric layer with a polymer is one way to enhance the flexibility. Yet, such a structure usually shows considerable anomalous dispersion by the lattice vibration of the dielectric layer in the IR regime[20,28]. In general, we control magnetic resonance by changing the geometrical factors. However, the resonance caused by lattice vibrations cannot be controlled because of the intrinsic properties of the materials. Some of research have suggested the thin film in the brittle part[22,23], however, the range of thickness is still thicker than the free of fracture[32]. Thus, we need to find other ways to overcome these conundrums for realizing flexible IR camouflage materials. In the engineering field, to release the stress concentrated at a certain point in a material, we change the structure of the material to reduce the strain at a fragile part, for example, by disconnecting or removing some parts, while maintaining its intrinsic functionality[33]. The reason is that the induced stress is the sum of structure distortions caused by constraints[34]. For this reason, we can apply this strategy for developing flexible metamaterials (FTCM) with a ceramic dielectric layer.

Herein, we developed FTCM for use as IR camouflage materials. On the basis of conventional IR camouflage materials, we disconnect the ceramic dielectric layer to release the mechanical stress caused by distortion. We present measurement and simulation results that EM behaviors of FTCM are similar to that of conventional IR camouflage materials. Furthermore, FTCM are free of angle dependence and temperature within the actual operational range. We quantified the IR camouflage performance of the FTCM in terms of

radiative energy, and the IR camouflage performance was comparable to that of conventional metamaterials. Finally, we confirmed that the FTCM could operate in a supersonic flowfield successfully despite high viscous shear force and severe temperature difference conditions.

2. Material and Methods

2.1. Simulation

For designing the FTCM, a numerical simulation was conducted using COMSOL Multiphysics v.5.2a with a wave optics module. The governing equation was Maxwell's equation and it was discretized for a finite element method. The unit cell of the FTCM was used in the simulation. The simulated domain consisted of a metal ground (Au), a dielectric layer (Si_3N_4), a metal disk (Au) and a medium (Air). The variables were the diameters of the dielectric layer and metal disk (D), the pitch of the unit cell (p) and the thickness of the dielectric layer (t_d). The relative permittivity, permeability and electrical conductivity in the medium were assumed to be 1, 1 and 0, respectively. The free electron behavior in the metal ground and disk (Au) was modelled using the Drude-Lorentz dispersion model, and the plasma frequency (2.06 PHz) and damping constant (13.34 THz)[12] were considered in the modelling. The dielectric layer was modelled by using its refractive index as a parameter[35]. The simulated wavelength ranged from 3 μm to 14 μm, and the grid size was restricted to 375 nm, which was determined by the grid independent test.

2.2. Fabrication

First, a 500 μm thick silicon wafer was cleaned with acetone, ethanol, and a buffered oxide etchant, with cleaning time of 10 min for each of the solutions, to remove the organic matters on the wafer. Subsequently, VTEC 1388 (liquid polyimide) was coated at 3000 rpm, resulting in the formation of a 13 μm polyimide substrate layer. This layer was cured at 80, 160 and 240°C, with a curing duration of 10 min at each of the temperatures. On the polyimide substrate, a 100 nm thick Au and a 10 nm thick with Ti layer (adhesive layer) were deposited using an electron beam evaporator (ULVAC, Japan) for use as a metal ground. A 100 nm thick silicon nitride layer was deposited by plasma-enhanced chemical vapour deposition (Plasma-Therm 790 Series). Subsequently, Au/Ti (100/10 nm) layers were again coated using an electron beam evaporator

(ULVAC, Japan). In order to prepare the disk patterns, a photoresist (AZ5214E) was coated using a spin coater (3000 rpm, 30 s), and lithography was then performed using a mask aligner (MA6, Karl SÜSS MicroTec SE, Germany). The disk's diameter was controlled by varying the dose rate (150–250 mJ/cm^2). For developing the mask pattern, we used MIF-300 for around 30 s with the duration depending on the developed pattern, and subsequently, an inductively couple plasma etcher (ICP, Oxford etcher, Oxford Instruments) was used to etch the metal disk and dielectric layers, except for the metal ground. Finally, we removed the photoresists in a plasma asher (100 W, 5 min) and stripped the external adhesive materials of the FTCM.

2.3. Measurement of infrared emissivity

To measure the spectral emissivity, we used Fourier transform infrared spectroscopy (FT-IR, Bruker Corp.). The beam splitter (KBr) induced a phase difference, and the measurement wavelength ranged from 1.3 μm to 27 μm. The reflectivity was measured by a reflection accessory (Bruker A513) on the basis of Kirchhoff's law[14], which is given by: $\varepsilon(\lambda) = \alpha(\lambda) = 1 - \rho(\lambda)$, with emissivity ε, absorptivity α, reflectivity ρ and wavelength λ, respectively. We ignored the transmissivity because of the presence of the metal ground in the FTCM. The signal ratio between the reference and the sample decided the reflectivity, that is, $\rho(\lambda) = S_{sample}(\lambda,T)/S_{reference}(\lambda,T)$ with reflected signal S and temperature T, respectively, assuming a constant temperature during the measurement. The reflection accessory also provided the directional reflectivity used in calculating the directional emissivity of the sample. The sample sizes were around 1.3 cm x 1.3 cm, and the reference reflectivity was measured by using a 200 nm thick Au surface.

The emissivity was also determined using an accessory (Bruker A540) that controlled the sample temperature between room temperature and 370°C. A deuterated L-alanine doped triglycine sulphate detector was used to observe the intensity from an emitting source. The emissivity was evaluated as the signal ratio between the reference and the sample: $S_{sample}(\lambda,T)/S_{ref}(\lambda,T) = \varepsilon_{sample}(\lambda,T)/\varepsilon_{ref}(\lambda,T)$; the reference signal was

determined by using a cavity blackbody (SR-200, CI Systems) whose temperature can be changed from 50 to 1200°C.

2.4. Thermographic and visible measurement

In order to observe IR radiation on human skin, we obtained a thermographic image using an IR camera (A655sc, FLIR Systems, Wilsonville, OR, US). The FTCM were fastened to human skin with scotch tape (3M). The processed emissivity of IR data was assumed to be 0.95. The visible image was used by a camera with specifications, 12 mega-pixel, f/1.5–2.4 aperture lens, 1.4 micron pixels and with optical image stabilization.

For the supersonic flow test, we attached the FTCM to mock-up surfaces with various curvatures by using adhesive tape. The thermographic image was measured by the IR camera (A655sc, FLIR Systems, Wilsonville, OR, US), and the visible image was measured by a camera with the specifications, 12 mega-pixel, f/1.7 aperture lens, 1.4 micron pixels and with optical image stabilization. A detailed description of the supersonic flow facility is presented in supplementary material.

3. Results

3.1. Flexible thermo-camouflage materials on an arbitrary surface

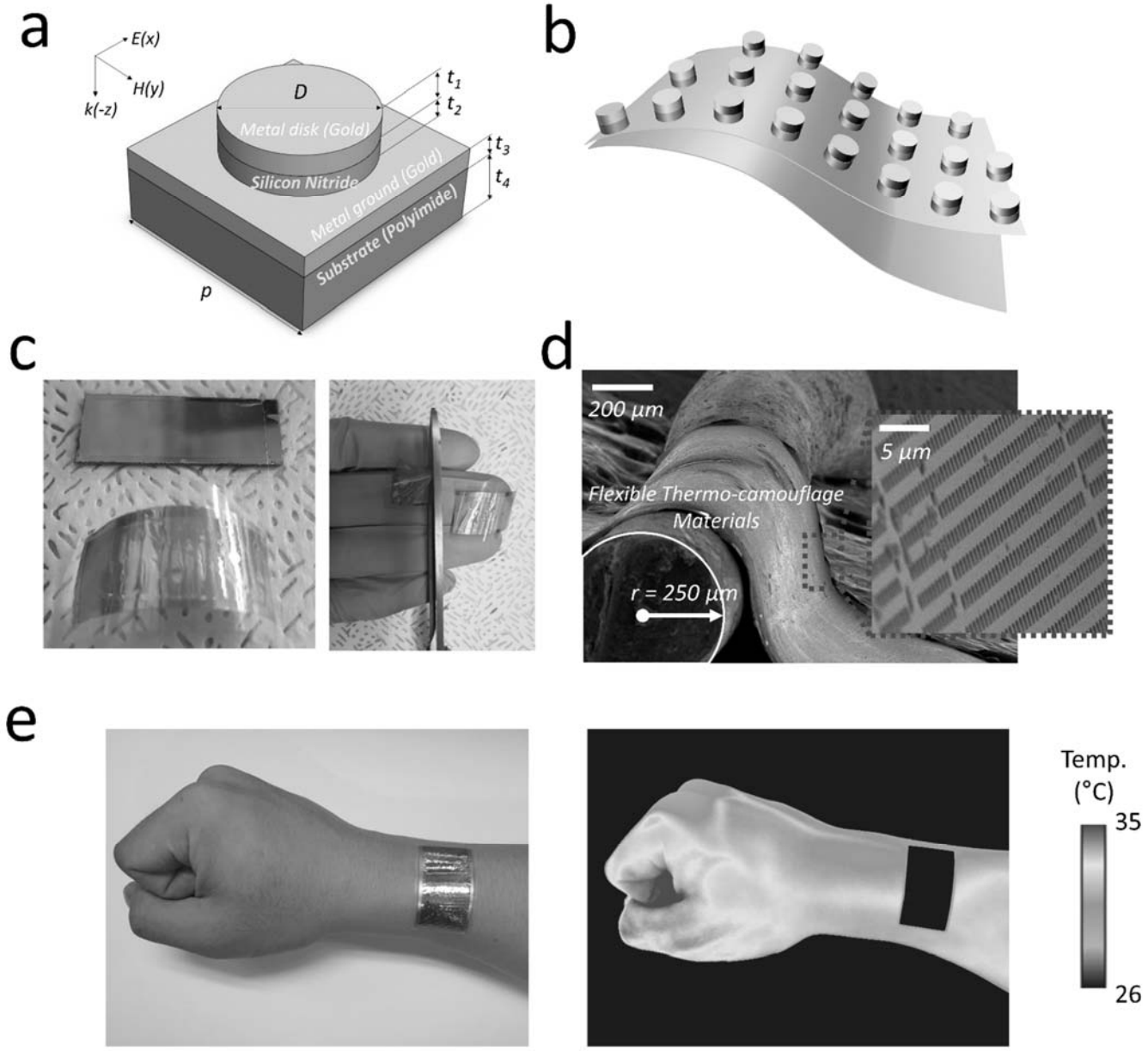

Figure 1. (a) Schematics of a unit cell and (b) an array of flexible thermo-camouflage materials (FTCM). FTCM consist of a substrate (polyimide), a metal ground (gold), a dielectric layer (silicon nitride) and a metal disk (gold). (c) Visible image of the FTCM showing the possibility of machining with scissors. (d) Scanning electron microscope image of the FTCM wrapped on a wire of radius 250 μm. (e) Qualitative evaluation of the IR camouflage performance of the FTCM (left: visible image; right: thermographic image (8-14 μm).

Figure 1(a) shows the unit cell of the FTCM having the conventional MDM structure. In case of asymmetric[36] and mixed shape[37], we can increase the operating band compared to the conventional emitter. However, in this study, we concentrate the material flexibility by disconnecting the brittle part in the MDM structure. Additionally, the fabrication is easier than the asymmetric shape. For this reason, as a shape of unit cell, we choose the circular shape which does not induce the polarization and the dependence on the incident angle against the IR detector. In case of FTCM, the substrate does not affect the EM behavior since, in the MDM structure, the metal ground (Au) blocks EM waves propagating toward the rear of the material. This means that we can choose the substrate material (polyimide) easily without considering the additional effect on the EM behavior of the FTCM. The dielectric layer, which is usually a ceramic material with brittle behavior, poses a problem, because it can endure only low strain in the material[32]. Therefore, we disconnect the dielectric layer reducing the maximum strain of dielectric layer to relieve the mechanical stress. Figures S1(a) and (b) show the mechanical stress distributions for a continuous and a discrete dielectric layer, as determined in a numerical simulation. The side walls are fixed, and the center part is deformed of 100 nm from the flat surface. Evidently, the mechanical stress in the discrete layer significantly decreases. To quantify the amount of reduction in the stress, we show the relative maximum stress in the dielectric part depending on the type of dielectric layer. In Fig. S1(c), the maximum stress after disconnecting the dielectric layer is 7.6% of that of the continuous dielectric layer. This implies that the discrete dielectric layer increases the mechanical reliability of the FTCM.

Additionally, we should consider the EM behaviors after disconnecting the dielectric layer which can cause the selective emission. The reason is that the change of effective permittivity by disconnecting a dielectric layer affects the EM behaviors as shown in Figs. S2(a) and (b). In Fig. S2(c), the spectral emissivity of the continuous and discrete dielectric layers is presented. Despite the difference between the dielectric layers, the discrete dielectric layer acts like the continuous dielectric layer in showing the selective emission. Therefore,

we infer that the unit cell structure in Fig. 1(a) acts like the conventional IR camouflage materials[17,18]. Based on the unit cell of FTCM, Fig.1(b) presents the schematic of FTCM arrays. We believe that FTCM can be flexible despite to irrespective of the curvature of its surface.

To use the FTCM in applications, it is important to detach it from the substrate (silicon wafer) without any mechanical failure. Figure 1(c) shows that the detachment can be easily achieved by using the adhesive tape from the substrate. Moreover, the camouflage target usually has a different size depending on its purpose, in which case the size of the FTCM would have to be modified. As shown in Fig. 1(c), the FTCM can be cut with conventional scissors. These results show that the FTCM can be used for any type of application by appropriately modifying its size. Furthermore, we should also need to evaluate the flexibility of FTCM. Figure 1(d) depicts a scanning electron microscope (SEM) image showing the curvature of the FTCM on a wire with a radius of 250 μm. We can observe that FTCM maintain the unit cell structure despite being wrapped on the wire, because of the reduced mechanical stress. This implies that having curvatures above a radius of 250 μm can be possible for enabling an arbitrary surface to be covered with the FTCM. Thus, the FTCM simultaneously possess machinability and flexibility, which can be manipulated depending on the purpose.

For checking the qualitative camouflage performance of the FTCM, we observed visible and IR images of the FTCM on the human arm representing various curvatures of the surface. The used adhesive material was scotch tape. In Fig. 1(e), the shining part is the FTCM acting as an IR camouflage material. Figure 1(e) shows that the FTCM are capable of IR camouflage. Except for covering area of scotch tape, which had a high emissivity ($\varepsilon > 0.8$), the FTCM provide a deceptive IR signature to the IR detector detecting in the range of 8–14 μm. The FTCM block the IR signature from the rear of signature, inducing a signature similar to that of the environment. This implies that the FTCM show IR camouflage performance as well as flexibility and machinability that facilitate the adjustment of its size to suit the arbitrary surface, unlike conventional

metamaterials. For further understanding of the FTCM, we should analyse its EM behaviors in the presence of IR waves through measurements and simulations.

3.2. Electromagnetic behavior of flexible thermo-camouflage materials

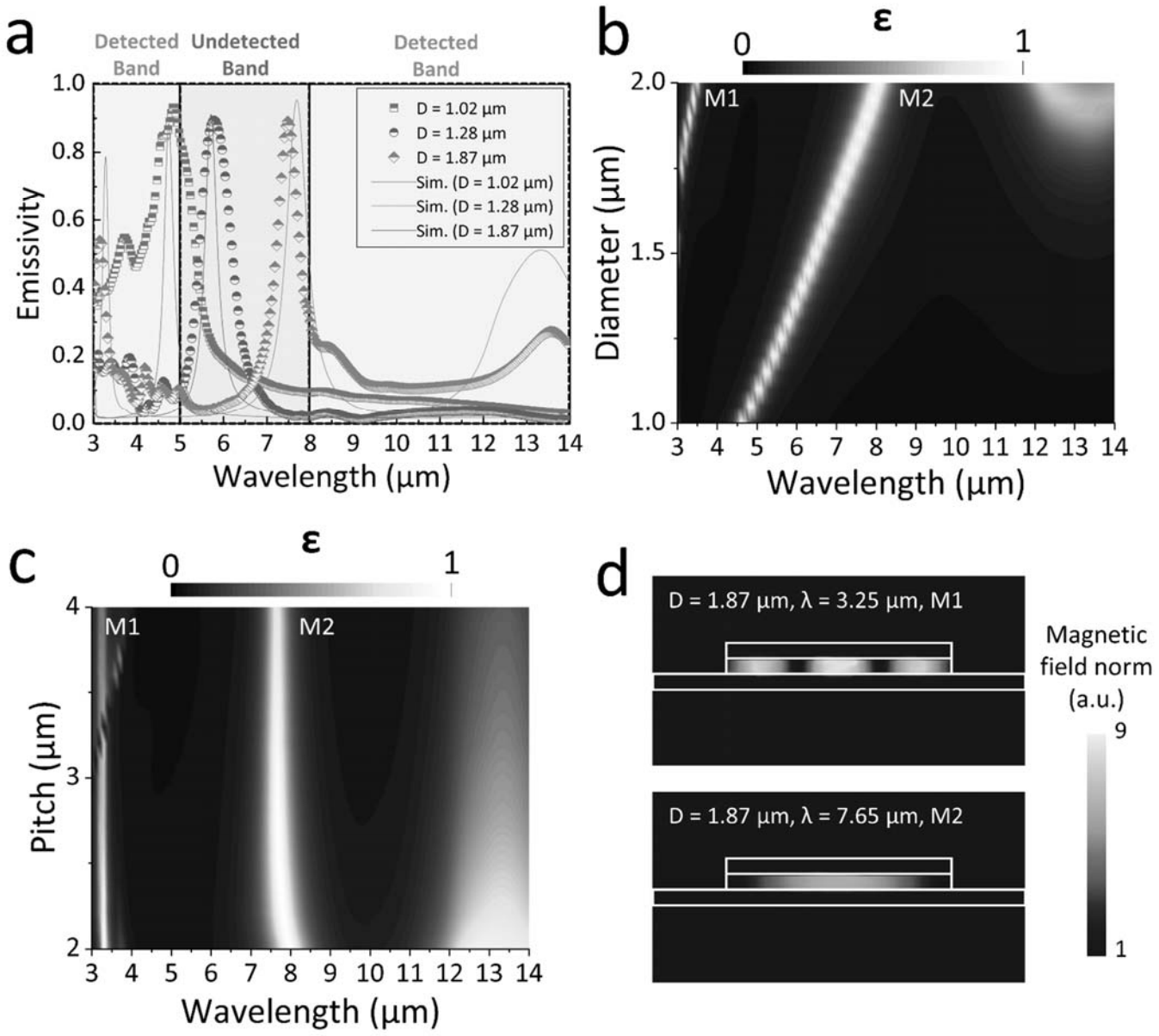

Figure 2. (a) Spectral emissivity of the FTCM in the range 3–14 μm. Scattered points are the emissivity values measured using Fourier-transform infrared (FT-IR) wave spectrometer. The line shows the results of a simulation performed using COMSOL Multiphysics v5.2. The green shaded areas indicate the detected bands (3–5 μm and 8–14 μm) and the blue shaded area represents the undetected band (5–8 μm). (b) Dependence of the simulated spectral emissivity on the diameter (D) of the unit cell from D = 1.0 μm to D = 2.0 μm. M1 and M2 denote magnetic resonance. (c) Dependence of the simulated spectral emissivity on the pitch (p) of the unit cell from p = 2.0 μm to p = 4.0 μm. (d) Visualization of the simulated magnetic resonance at M1 and M2.

As mentioned, for IR camouflage, the spectral emissivity in the detected bands (3–5, 8–14 μm) is sufficiently small enough to hide the IR signature from the target and that in the undetected band (5–8 μm) is sufficiently high to dissipate the accumulated radiative energy due to the reduced IR signature. Figure 2(a) shows the spectral emissivity of the FTCM for different diameters of the metal and dielectric disks. The fabricated structures are presented in Fig. S3. Selective emission occurs at 4.9 μm, 6.0 μm and 7.5 μm for diameters (D) of 1.02 μm, 1.28 μm and 1.87 μm, respectively. This implies that the resonant wavelength can be controlled by varying the diameter of a unit cell. In a previous study, for maximizing the IR camouflage performance, the authors set the resonant wavelength in the range 7–8 μm, since the temperature in a typical environment (30-200°C) causes the maximum energy dissipation in the range 6–10 μm according to Wien's displacement law[14]. Thus, the FTCM have an appropriate resonant wavelength as an IR camouflage material.

To further understand the EM behaviors of FTCM, we should analyse the dependence of geometrical factors on the spectral emissivity. Such an analysis can provide information about localized and non-localized plasmon behavior[30,38]. Typically, the localized plasmon behavior depends on the diameter of the unit cell, which is related to the magnetic resonance. By contrast, the non-localized plasmon behavior depends on the pitch of the unit cell, which is related to the surface plasmon or anomalous dispersion by the lattice vibration. Figures 2(b) and (c) show the variation of spectral emissivity with the diameter (p = 3 μm) and pitch (D = 1.87 μm), respectively. In Figs. 2(b) and (c), two resonant wavelengths can be observed at M1 (3–4 μm) and M2 (5–8 μm). As mentioned, these resonances are an aspect of the localized plasmonic behaviors, which is related to the magnetic resonance in the dielectric layer. Figure 2(d) shows simulated magnetic fields inside the unit cell of FTCM. At M1, a higher order of magnetic resonance is observed, which is natural behavior when exposed by the shorter wavelength of sub-micron MDM structure[17]. At M2, a magnetic resonance occurs in the unit cell, which is the main resonance of selective emission that we desired. This EM behavior is identical to that

of a conventional selective emitter in previous works[17,18]. In order to control the selective emission for other applications, we could obtain an M2 peak matching the desired wavelength.

The EM behavior around 13 μm is interesting, and it is related to the EM property of the dielectric layer despite the weak resonance. Except for ZnS, dielectric materials usually show anomalous dispersion in IR spectrum, which induces the additional resonances by the lattice vibration. This anomalous dispersion is expressed by varying the complex refractive index. In general, the real part of refractive index (n) dominates the impedance matching of materials and the imaginary part of refractive index (k) relates to the absorption coefficient of materials[39]. The effect of n on impedance matching is manifest, but the effect of k is insufficient to explain the EM behaviors on the materials because its value is small. To ascertain the effect of k, we simulated the EM behaviors depending on $k = 0$ or intrinsic values[35]. In Fig. S4, the spectral emissivity for $k = 0$ is similar to that at resonant wavelength of 13.25 μm observed in the experimental results. It means that the increase of n, anomalous dispersion, induces the additional impedance matching at 13.25 μm. Since the effect of k is related to the thickness which increases the absorption in a dielectric layer, it affects the spectral emissivity only slightly because of thin thickness (100 nm) of dielectric layer. Additionally, in MDM structure, the cause of resonant behavior happens inside metal parts[40] in terms of energy dissipation. For this reason, k is little impact on FTCM' spectral emissivity. In the aspect of IR camouflage, however, the effect of anomalous dispersion is little enough to reduce the IR signature from the rear side, resulting in ignoring this EM behavior as IR camouflage materials.

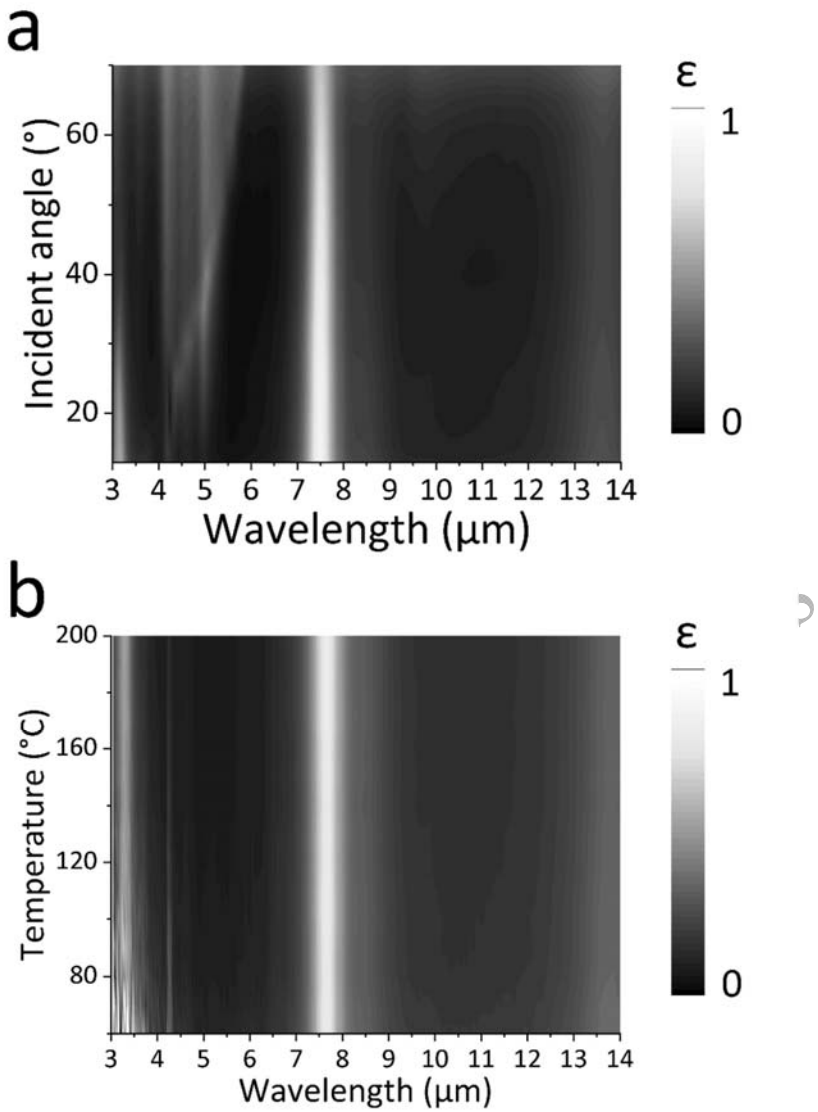

Figure 3. Dependence of the measured spectral emissivity of the FTCM on the (a) incident angle and (b) temperature. The unit cell of the FTCM has the parameters D = 1.87 μm and p = 3.0 μm.

To consider the possible use of the FTCM in severe condition, we should consider the incident angle and temperature dependence on the IR camouflage performance of the FTCM. Figure 3(a) shows the dependence of the spectral emissivity on the incident angle. It shows that selective emission occurs up to 60° when a low spectral emissivity is maintained in the detected bands. This result is important since the detector can seek the

target by varying the incident angle. For a cylindrical shape, 60° can cover 66% of the surface. This implies that the susceptibility of the target is sufficiently reduced to improve the survivability of target[41]. In addition, the surface temperature can increase up to 180°C, which is the total temperature of Mach number = 2.0 at an altitude of 5000 m. Figure 3(b) shows the temperature dependence of the spectral emissivity. Clearly, the spectral emissivity is independent of the temperature despite the temperature reaching 200°C. The constituent materials of FTCM are gold, silicon nitride and polyimide. The polyimide typically endures temperatures up to 200°C[42], which indicates that we can utilize the FTCM in the operating condition up to the Mach number = 2.0 at an altitude of 5000 m which is harsh condition of the aircraft.

3.3. Thermal (IR) camouflage performance of FTCM

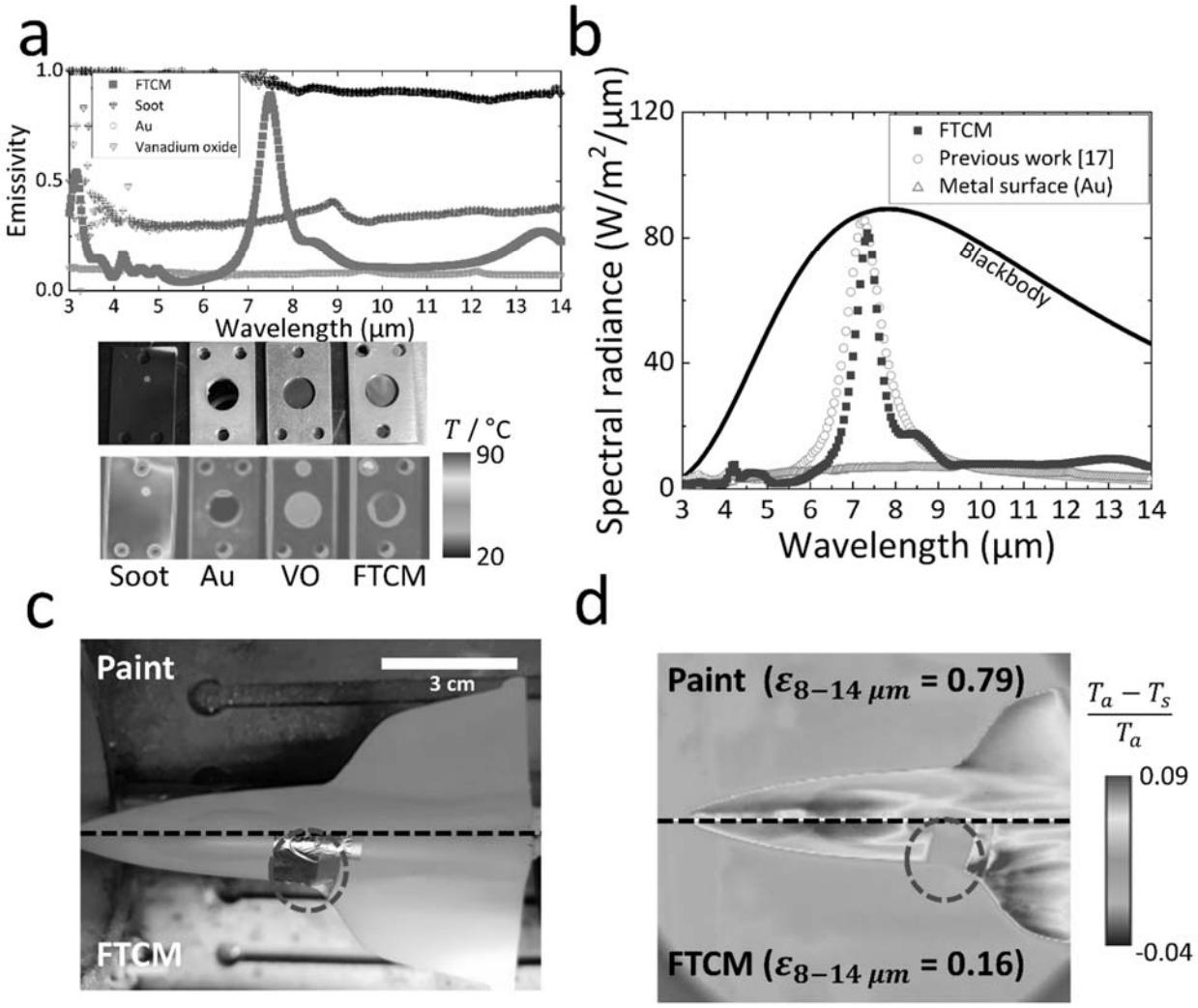

Figure 4. (a) Spectral emissivity and IR images of several surfaces such as Au, FTCM, Soot and Vanadium oxide (VO). The heated surface temperature is 370 K which is controlled by the heating plate. (b) Spectral radiance of the FTCM, conventional IR camouflage materials and blackbody. (c) Visible image of the mock-up with various curvatures and wrapped with the FTCMs in the test section. The scale bar represents 3 cm. (d) Comparison of thermographic image of the mock-up in the supersonic flowfield between the gray paint and the FTCMs in the center part. T_s and T_a are the surface temperature and the ambient temperature, respectively. T_a is 290 K controlled by the air-conditioning system. The video clip of thermographic image with FTCMs is provided in the supplementary files.

On the basis of the basic understanding of EM behavior of the FTCM, we quantify the variation of radiative energy in the detected and undetected bands for evaluating the IR camouflage performance. Firstly, we

compare IR images such as Au, Soot, Vanadium oxide (VO) and FTCM. The measured spectral emissivity is presented in Fig. 4(a). Au and Soot surface presents the lowest and highest emissivity in infrared regime (3-14 μm), respectively. Vanadium oxide is a reference surface which is used for the radiation control surface[43], which value is 0.4 in infrared regime. The IR image in 8-14 μm shows that the apparent temperature of FTCM is close to the Au surface compared to VO. It means that FTCM is higher camouflage performance than VO.

Secondly, by assuming diffusive emission from the surface, we can evaluate the spectral irradiance of a blackbody using following equation[14]:

$$E_{b\lambda}(\lambda, T) = \frac{2\pi h c_0^2}{\lambda^5 \left[\exp[\frac{hc_0/k}{\lambda T} - 1]\right]} \quad (1)$$

where h, c_0, k and T are Planck's constant, the speed of light in vacuum, Boltzmann's constant, and the temperature, respectively. For obtaining the radiative energy from the spectral irradiance, we should integrate the spectral irradiance along with the wavelength in certain bands. If the bands range from λ_1 to λ_2, the integration can be expressed as:

$$E_{\lambda_1-\lambda_2}(T) = \int_{\lambda_1}^{\lambda_2} \varepsilon(\lambda, T)\, E_{b\lambda}(\lambda, T)\, d\lambda \cong \sum \varepsilon(\lambda, T)\, E_{b\lambda}(\lambda, T)\Delta\lambda \quad (2)$$

where ε is the measured emissivity of materials. Using Eq. (2), we evaluate the variation of the radiative energy due to the FTCM.

Figure 4(b) shows the spectral radiance of a blackbody, a metal, a conventional metamaterial and the FTCM. The blackbody surface is the best for energy dissipation in the undetected band, but the worst for IR camouflage in the detected band since the radiative energy is maximized. The metal surface is ideal for reducing the radiative energy in the detected bands, but the worst surface for energy dissipation in the undetected band. In this study, we chose gold as the metal surface. Gold has been widely studied for use on IR camouflage surface[44,45]. The temperature of the target surface is assumed to be 370 K on the basis of the calculated value

of the total temperature at the altitude of 5000 m and Mach number = 1.5. In the detected bands, the blackbody emits 47.3 W/m^2 in the range 3–5 μm and 421.6 W/m^2 in the range 8–14 μm. The FTCM emit 5.5 W/m^2 and 65.5 W/m^2 in these two ranges, respectively, implying that their radiative energies are 12% (3–5 μm) and 16% (8–14 μm) of the blackbody's signature, respectively. It means that the wideband emissivity in 3–5 μm and 8–14 μm are 0.12 and 0.16, respectively. These values are similar to the conventional emitter which are 15% and 11% of blackbody's radiative energy in the ranges of 3–5 μm ($\varepsilon_{3\text{-}5\ \mu m}$ = 0.15) and 8–14 μm ($\varepsilon_{8\text{-}14\ \mu m}$ = 0.11), respectively. At the same condition, the metal surface shows radiative energies that 9% and 8% of blackbody's radiative energy in the ranges of 3–5 μm ($\varepsilon_{3\text{-}5\ \mu m}$ = 0.09) and 8–14 μm ($\varepsilon_{8\text{-}14\ \mu m}$ = 0.08), respectively. These results show that, similar to the conventional camouflage material and metal surface, the FTCM can hide the IR signature from its surface, successfully.

The metal surface dissipates 17.6 W/m^2 in the range 5–8 μm while maintaining IR camouflage in the detected bands. In the case of the FTCM, the dissipative energy and wideband emissivity in the undetected band is 63.1 W/m^2 and 0.27, which is 2580% greater than that of the metal surface. Even though conventional metamaterials (98.7 W/m^2 and 0.42) show 36% higher energy dissipation compared with the FTCM, we think that the FTCM have camouflage performance comparable to that of a conventional camouflage surface because of its flexibility and machinability.

Finally, we attempted to determine the FTCM's camouflage performance against the IR detector under severe flow conditions such as those in a supersonic flowfield. The supersonic wind tunnel induced a Mach number = 3.0 with the high shear force. The total temperature of working fluid is 290 K and the static temperature in Mach number 3.0 is 104 K. A detailed description of the experimental facility is provided in Fig. S5. Figure 4(c) shows the mock-up of the target surface wrapped with the FTCM. As shown in Fig. 4(b), the FTCM can be fastened to a curved surface without any problems, despite the curvature of its surface varying with its location. Figure 4(d) shows the IR image of the mock-up wrapped with the FTCM. In Fig.

4(d), the wrapped part is assimilated with the environment and hides its IR signature against the IR detector. In the case of the bare surface coated with paint, the IR signature is different from the background, which leads to the higher susceptibility of the target against the IR detector. Moreover, during the operation, the FTCM maintain the IR camouflage performance. This means that the FTCM had high durability against the high viscous shear force in the supersonic flowfield including shock waves and successfully maintained IR camouflage under the operating conditions.

4. Conclusion

We verified that the FTCM showed IR camouflage on an arbitrary surface without mechanical failure. Without using a polymer as a dielectric layer, we realized a flexible structure by changing the unit cell structure. On the basis of SEM, visible and IR images, we confirmed the machinability, flexibility and IR camouflage performance of the FTCM. Measurements and simulations indicated that the FTCM showed EM behaviors similar to that of conventional camouflage materials. Moreover, the FTCM are independent of the incident angle of IR waves and temperature under the operating conditions considered in this study. We quantified the IR camouflage performance of the FTCM; its energy dissipation was 2580% higher than that of the metal surface (Au) in the undetected band (5–8 μm) and its radiative energy was lower than the blackbody's radiative energy by 12% and 16% in the detected bands (3–5 μm and 8–14 μm), respectively. Additionally, the reduced radiative energy of the FTCM was comparable to the radiative energy of conventional metamaterials and the metal surface. Finally, in the supersonic flow test, we confirmed the IR camouflage performance of the FTCM on an arbitrary surface.

Unlike the existing flexible materials, the FTCM can be fabricated using the conventional procedure of MEMS fabrication without requiring any additional special process. In contrast to previous flexible materials using a polymer dielectric layer, the FTCM show EM behavior similar to that of a conventional camouflage material because of its the conventional MDM structure. Although, in order to utilize this material for the actual applications, the mechanical reliability should be secured against the mechanical perturbation such as rubbing and scratching, we expect that the FTCM can substitute MDM-structured materials in applications typical of the MDM structure, such as radiative cooling, energy conversion, and space applications through the additional structure to protect the micro-nano structure which is fragile against the external perturbation. The FTCM have the potential to help improve our understanding of the basic characteristics of the MDM structure and to contribute to the development of metamaterials for real applications.

Associated Content

Supporting information

Simulation of mechanical stress on a flexible thermo-camouflage materials (FTCM), Simulation of the effect of the structure of the dielectric layer on spectral emissivity, Scanning electron microscope (SEM) image of fabricated FTCM, Simulated results of the effect of imaginary part of refractive index on spectral emissivity of FTCM, Description of supersonic flow tunnel for evaluating the IR camouflage performance

Author Information

Corresponding Author

*E-mail: hhcho@yonsei.ac.kr

Author contributions

N. L., and H. H. C. designed the overall strategy. N. L., J.-S. L. and D. L. fabricated the specimen and measured the spectral emissivity through a FT-IR facility. N. L. and I. C. performed the numerical simulation for revealing the electromagnetic behaviors. J.-S. L. and I. C. captured the visible and infrared images to evaluate the camouflage performance. All the authors analyzed the data. N. L. and H. H. C. wrote and supervise the manuscript.

Acknowledgements

This work was supported by the Aerospace Low Observable Technology Laboratory Program of the Defense Acquisition Program Administration and the Agency for Defense Development of the Republic of Korea.

References

(1) Xu, C.; Colorado Escobar, M.; Gorodetsky, A. A. Stretchable Cephalopod-Inspired Multimodal Camouflage Systems. *Adv. Mater.* **2020**, *32* (16), e1905717.

(2) Barnett, J. B.; Michalis, C.; Anderson, H. M.; McEwen, B. L.; Yeager, J.; Pruitt, J. N.; Scott-Samuel, N. E.; Cuthill, I. C. Imperfect Transparency and Camouflage in Glass Frogs. *Proc. Natl. Acad. Sci. U. S. A.* **2020**, *117* (23), 12885–12890.

(3) Morin, S. A.; Shepherd, R. F.; Kwok, S. W.; Stokes, A. A.; Nemiroski, A.; Whitesides, G. M. Camouflage and Display for Soft Machines. *Science* **2012**, *337* (6096), 828–832.

(4) Phan, L.; Walkup, W. G.; Ordinario, D. D.; Karshalev, E.; Jocson, J.-M.; Burke, A. M.; Gorodetsky, A. A. Reconfigurable Infrared Camouflage Coatings from a Cephalopod Protein. *Adv. Mater.* **2013**, *25* (39), 5621–5625.

(5) Leung, E. M.; Colorado Escobar, M.; Stiubianu, G. T.; Jim, S. R.; Vyatskikh, A. L.; Feng, Z.; Garner, N.; Patel, P.; Naughton, K. L.; Follador, M.; Karshalev, E.; Trexler, M. D.; Gorodetsky, A. A. A Dynamic Thermoregulatory Material Inspired by Squid Skin. *Nat. Commun.* **2019**, *10* (1), 1947.

(6) Lenert, A.; Bierman, D. M.; Nam, Y.; Chan, W. R.; Celanović, I.; Soljačić, M.; Wang, E. N. A Nanophotonic Solar Thermophotovoltaic Device. *Nat. Nanotechnol.* **2014**, *9* (2), 126–130.

(7) Wang, H.; Chang, J.-Y.; Yang, Y.; Wang, L. Performance Analysis of Solar Thermophotovoltaic Conversion Enhanced by Selective Metamaterial Absorbers and Emitters. *Int. J. Heat Mass Transf.* **2016**, *98*, 788–798.

(8) Raman, A. P.; Anoma, M. A.; Zhu, L.; Rephaeli, E.; Fan, S. Passive Radiative Cooling below Ambient Air Temperature under Direct Sunlight. *Nature* **2014**, *515* (7528), 540–544.

(9) Li, M.; Coimbra, C. F. On the Effective Spectral Emissivity of Clear Skies and the Radiative Cooling Potential of Selectively Designed Materials. *Int. J. Heat Mass Trans.* **2019**, *135*, 1053–1062.

(10) Trosseille, J.; Mongruel, A.; Royon, L.; Beysens, D. Radiative Cooling for Dew Condensation. *Int. J. Heat Mass Transf.* **2021**, *172*, 121160.

(11) Pech-May, N.W.; Lauster, T.; Retsch, M. Design of Multimodal Absorption in the Mid-IR: A Metal Dielectric Metal Approach. *ACS Appl. Mater. Interf.* **2021**, *13* (1), 1921-1929.

(12) Liu, N.; Mesch, M.; Weiss, T.; Hentschel, M.; Giessen, H. Infrared Perfect Absorber and Its Application as Plasmonic Sensor. *Nano Lett.* **2010**, *10* (7), 2342–2348.

(13) Luo, H.; Li, Q.; Du, K.; Xu, Z.; Zhu, H.; Liu, D.; Cai, L.; Ghosh, P.; Qiu, M. An Ultra-thin Colored Textile with Simultaneous Solar and Passive Heating Abilities. *Nano Energy* **2019**, *65*, 103998.

(14) Cengel, Y. *Heat and mass transfer: fundamentals and applications*; McGraw-Hill Higher Education, 2014.

(15) Lee, J.; Sul, H.; Jung, Y.; Kim, H.; Han, S.; Choi, J.; Shin, J.; Kim, D.; Jung, J.; Hong, S.; Ko, S. H. Thermally Controlled, Active Imperceptible Artificial Skin in Visible-to-Infrared Range. *Adv. Funct. Mater.* **2020**, *30* (36), 2003328.

(16) Hong, S.; Shin, S.; Chen, R. An Adaptive and Wearable Thermal Camouflage Device. *Adv. Funct. Mater.* **2020**, *30* (11), 1909788.

(17) Kim, T.; Bae, J.-Y.; Lee, N.; Cho, H. H. Hierarchical Metamaterials for Multispectral Camouflage of Infrared and Microwaves. *Adv. Funct. Mater.* **2019**, *29* (10), 1807319.

(18) Lee, N.; Kim, T.; Lim, J.-S.; Chang, I.; Cho, H. H. Metamaterial-Selective Emitter for Maximizing Infrared Camouflage Performance with Energy Dissipation. *ACS Appl. Mater. Interf.* **2019**, *11* (23), 21250–21257.

(19) Lee, N.; Lim, J.-S.; Chang, I.; Lee, D.; Cho, H. H. Transparent Metamaterials for Multispectral Camouflage Transparent Metamaterials for Multispectral Camouflage with Thermal Management. *Int. J. Heat Mass Transf.* **2021**, *173*, 121173.

(20) Lee, N.; Yoon, B.; Kim, T.; Bae, J.-Y.; Lim, J.-S.; Chang, I.; Cho, H. H. Multiple Resonance Metamaterial Emitter for Deception of Infrared Emission with Enhanced Energy Dissipation. *ACS Appl. Mater. Interf.* **2020**, *12* (7), 8862–8869.

(21) Zhu, H.; Li, Q.; Zheng, C.; Hong, Y.; Xu, Z.; Wang, H.; Shen, W.; Kaur, S.; Ghosh, P.; Qiu, M. High-Temperature Infrared Camouflage with Efficient Thermal Management. *Light Sci. Appl.* **2020**, *9*, 60.

(22) Zhu, H.; Li, Q.; Tao, C.; Hong, Y.; Xu, Z.; Shen, W.; Kaur, S.; Ghosh, P.; Qiu, M. Multispectral Camouflage for Infrared, Visible, Lasers and Microwave with Radiative Cooling. *Nat. Commun.* **2021**, *12*(1), 1805.

(23) Peng, L.; Liu, D.; Cheng, H.; Zhou, S.; Zu, M. A Multilayer Film Based Selective Thermal Emitter for Infrared Stealth Technology. Advanced Optical Materials 2018, 6 (23), 1801006. DOI: 10.1002/adom.201801006.

(24) Sheehan, D. P. Infrared Cloaking, Stealth, and the Second Law of Thermodynamics. *Entropy* **2012**, *14* (10), 1915–1938.

(25) Harris, D. C. *Materials for Infrared Windows and Domes: Properties and Performance*; SPIE, 1999.

(26) Pan, M.; Huang, Y.; Li, Q.; Luo, H.; Zhu, H.; Kaur, S.; Qiu, M. Multi-Band Middle-Infrared-Compatible Camouflage with Thermal Management via Simple Photonic Structures. *Nano Energy* **2020**, *69*, 104449.

(27) Salihoglu, O.; Uzlu, H. B.; Yakar, O.; Aas, S.; Balci, O.; Kakenov, N.; Balci, S.; Olcum, S.; Süzer, S.; Kocabas, C. Graphene-Based Adaptive Thermal Camouflage. *Nano Lett.* **2018**, *18* (7), 4541–4548..

(28) Jiang, Z. H.; Yun, S.; Toor, F.; Werner, D. H.; Mayer, T. S. Conformal Dual-Band Near-Perfectly Absorbing Mid-Infrared Metamaterial Coating. *ACS Nano* **2011**, *5* (6), 4641–4647.

(29) Kazemi Moridani, A.; Zando, R.; Xie, W.; Howell, I.; Watkins, J. J.; Lee, J.-H. Plasmonic Thermal Emitters for Dynamically Tunable Infrared Radiation. *Adv. Opt. Mater.* **2017**, *5* (10), 1600993.

(30) Dao, T. D.; Chen, K.; Ishii, S.; Ohi, A.; Nabatame, T.; Kitajima, M.; Nagao, T. Infrared Perfect Absorbers Fabricated by Colloidal Mask Etching of Al–Al2O3–Al Trilayers. *ACS Photon.* **2015**, *2* (7), 964–970.

(31) Üstün, K.; Turhan-Sayan, G. Wideband Long Wave Infrared Metamaterial Absorbers Based on Silicon Nitride. *J. Appl. Phys.* **2016**, *120* (20), 203101.

(32) Luo, J.; Wang, J.; Bitzek, E.; Huang, J. Y.; Zheng, H.; Tong, L.; Yang, Q.; Li, J.; Mao, S. X. Size-Dependent Brittle-to-Ductile Transition in Silica Glass Nanofibers. *Nano Lett.* **2016**, *16* (1), 105–113.

(33) Norajitra, P. *Divertor Development for a Future Fusion Power Plant*; Schriftenreihe des Instituts für Angewandte Materialien, Vol. 1; KIT Scientific Publishing, 2011.

(34) M Gere, J. *Mechanics of Materials Sixth Edition*; Copyright, 2004.

(35) Kischkat, J.; Peters, S.; Gruska, B.; Semtsiv, M.; Chashnikova, M.; Klinkmüller, M.; Fedosenko, O.; Machulik, S.; Aleksandrova, A.; Monastyrskyi, G.; Flores, Y.; Masselink, W. T. Mid-Infrared Optical Properties of Thin Films of Aluminum Oxide, Titanium Dioxide, Silicon Dioxide, Aluminum Nitride, and Silicon Nitride. *Appl. Opt.* **2012**, *51* (28), 6789–6798.

(36) Liu, B.; Gong, W.; Yu, B.; Li, P.; Shen, S. Perfect Thermal Emission by Nanoscale Transmission Line Resonators. *Nano Lett.* **2017**, *17* (2), 666–672.

(37) Maremi, F.; Lee, N.; Choi, G.; Kim, T.; Cho, H. Design of Multilayer Ring Emitter Based on Metamaterial for Thermophotovoltaic Applications. *Energies* **2018**, *11* (9), 2299.

(38) T. A. Kelf; Y. Sugawara; R. M. Cole; J. J. Baumberg; M. E. Abdelsalam; S. Cintra; S. Mahajan; A. E. Russell; P. N. Bartlett. Localized and Delocalized Plasmons in Metallic Nanovoids. *Phys. Rev. B* **2006**, *74* (24), 245415.

(39) Hecht, E. *Optics*; Addison Wesley San Francisco, 2002.

(40) Vora, A.; Gwamuri, J.; Pala, N.; Kulkarni, A.; Pearce, J. M.; Güney, D. Ö. Exchanging Ohmic Losses in Metamaterial Absorbers with Useful Optical Absorption for Photovoltaics. *Sci. Rep.* **2014**, *4*, 4901.

(41) Kim, T.; Lee, H.; Bae, J.-Y.; Kim, T.; Cha, J.; Jung, D.; Cho, H. H. Susceptibility of Combat Aircraft Modeled as an Anisotropic Source of Infrared Radiation. *IEEE Trans. Aerosp. Electron. Syst.* **2016**, *52* (5), 2467–2476..

(42) Liaw, D.-J.; Wang, K.-L.; Huang, Y.-C.; Lee, K.-R.; Lai, J.-Y.; Ha, C.-S. Advanced Polyimide Materials: Syntheses, Physical Properties and Applications. *Prog. Polymer Sci.* **2012**, *37* (7), 907–974.

(43) Kats, M. A.; Blanchard, R.; Zhang, S.; Genevet, P.; Ko, C.; Ramanathan, S.; Capasso, F. Vanadium Dioxide as a Natural Disordered Metamaterial: Perfect Thermal Emission and Large Broadband Negative Differential Thermal Emittance. *Phys. Rev. X* **2013**, *3* (4), 041004.

(44) Ting, T.-H.; Wu, K.-H.; Hsu, J.-S.; Chuang, M.-H.; Yang, C.-C. Microwave Absorption and Infrared Stealth Characteristics of Bamboo Charcoal/Silver Composites Prepared by Chemical Reduction Method. *J. Chin. Chem. Soc.* **2008**, *55* (4), 724–731.

(45) Tian, H.; Liu, H.-T.; Cheng, H.-F. A Thin Radar-Infrared Stealth-Compatible Structure: Design, Fabrication, and Characterization. *Chin. Phys. B* **2014**, *23* (2), 25201.

Table of Contents

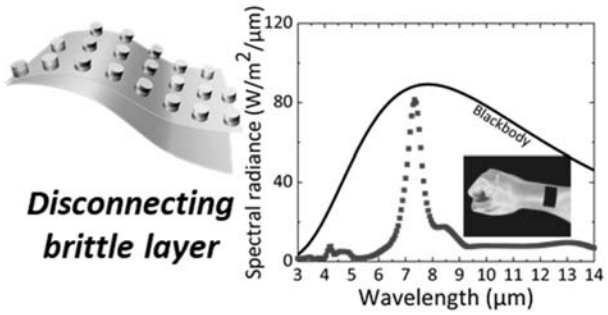

Supporting Information

Flexible Thermo-Camouflage Materials in Supersonic Flowfields with Selective Energy Dissipation

Namkyu Lee[a], Joon-Soo Lim[b], Injoong Chang[b], Donghwi Lee[c], Hyung Hee Cho[b,*]

a. IBI-4, Forschungszentrum Jülich GmbH, 52425 Jülich, Germany

b. Department of Mechanical Engineering, Yonsei University, 50 Yonsei-ro, Seodaemun-gu, Seoul 13722, Korea

c. Department of Mechanical Engineering, University of Wisconsin–Madison, 1500 Engineering Drive, Madison, WI 53706, United States

* Corresponding author

Tel.: +82 2 2123 2828

Fax: +82 2 312 2159

E-mail: hhcho@yonsei.ac.kr

1. Simulation of mechanical stress on a flexible thermo-camouflage materials (FTCM)

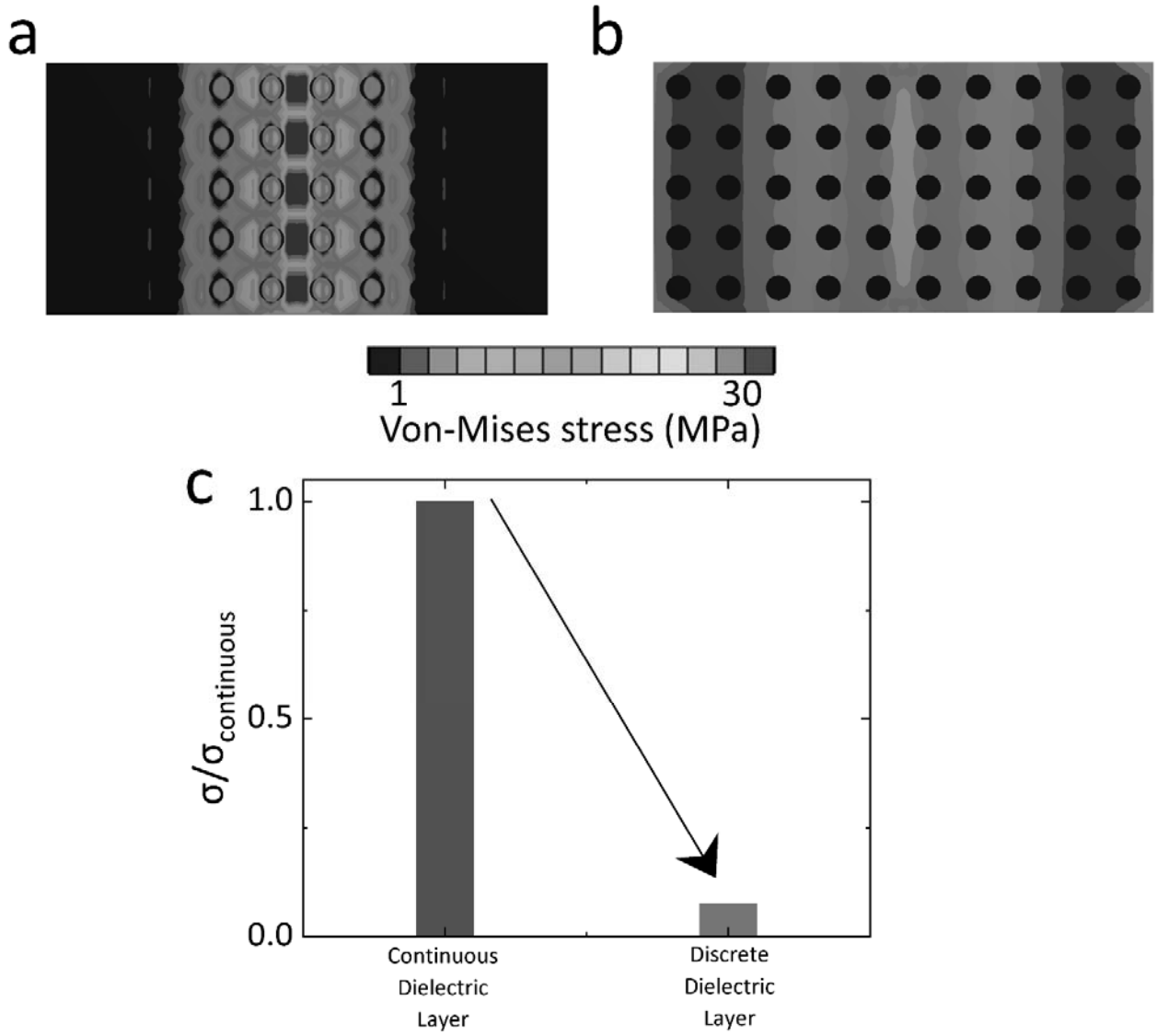

Figure S1. Simulation results of the von-Mises stress distribution of (a) a continuous dielectric layer and (b) a discrete dielectric layer. (c) Comparison of the relative maximum stress in a dielectric layer depending on the continuous and discrete structure

For analysing the mechanical stress associated with the structure of the dielectric layer, we calculate the mechanical stress using a commercial solver of ANSYS v15.0. The simulated geometry consists of three parts:

a metal ground, a dielectric layer, and a metal disk. The substrate of polyimide is removed because it has high flexibility compared to the other materials. Both edges at the bottom layer are fixed, and the centre part change 100 nm from the original surface. Figures S1 (a) and (b) show the mechanical stress distribution for the continuous and discrete dielectric layers, respectively. The mechanical stress is evaluated using the von-Mises stress, expressed as follows:

$$\sigma_{Von-Mises} = \sqrt{\frac{(\sigma_x - \sigma_y)^2 + (\sigma_y - \sigma_z)^2 + (\sigma_z - \sigma_x)^2}{2} + 3(\tau_{xy}^2 + \tau_{yz}^2 + \tau_{zx}^2)} \quad (1)$$

where σ and τ are the normal and shear stress, respectively. One of these stresses is used to evaluate the mechanical durability [1]. As shown in Figs. S1(a) and (b), the stress in the discrete layer is considerably reduced. The reason is that the disconnection induces lower distortion in the dielectric layer, resulting in the lower stress in the structure. To quantify the variation of stress, we calculate the relative stress on the basis of the maximum stress of the continuous dielectric layer. It is observed that the maximum stress in the discrete case is 7.4% of that in the continuous case. This proves that in the discrete layer, the maximum stress is significantly reduced.

2. Effect of the structure of the dielectric layer on spectral emissivity

Figure S2 compares the spectral emissivity for the discrete and continuous dielectric layers of the FTCM. The simulation is performed using a commercial solver of COMSOL Multiphysics v.5.2 with Optics Module. As shown in Fig. S2, the EM behavior is similar despite the difference between the dielectric layers. In general, when increasing the thickness of dielectric layer on a metal-dielectric-metal structure, the peak resonance has a red shift that moves the resonance peak toward longer wavelengths. We thought that the atmospheric environment also acts like a dielectric layer that induces the smaller effective permittivity of dielectric layer of FTCM, which causes the blue shift. Therefore, we are convinced that the discrete layer can be used in the FTCM intended for IR camouflage.

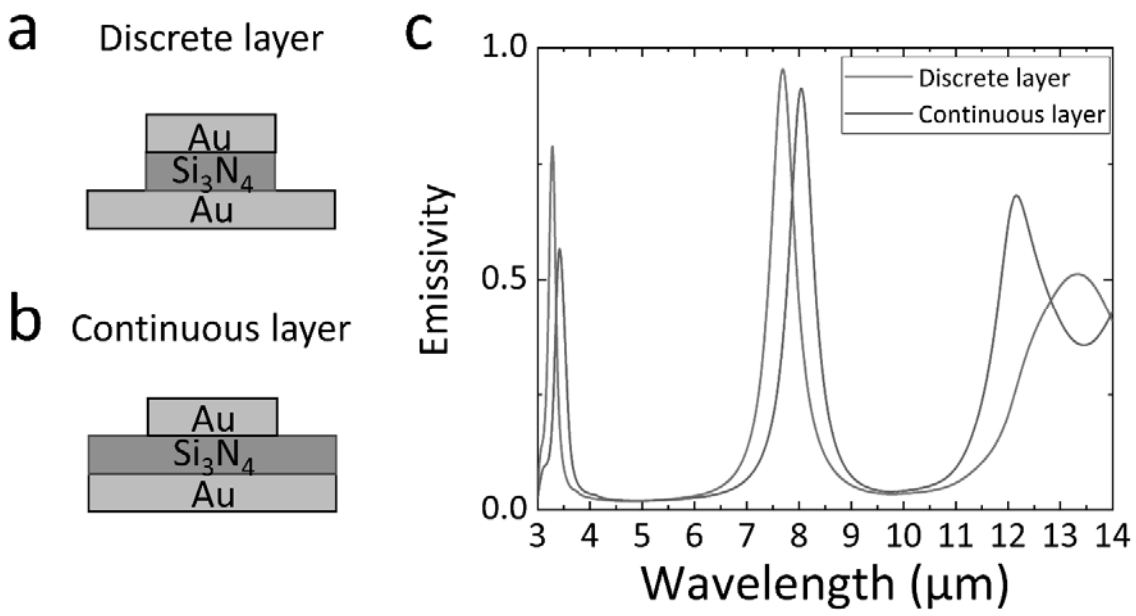

Figure S2. Schematics of (a) discrete and (b) continuous dielectric layer. (c) Simulated spectral emissivity of the discrete and continuous dielectric layers (D = 1.87 μm, p = 3 μm).

3. Scanning electron microscope (SEM) image of fabricated FTCM

Figure S3 shows an SEM image of the fabricated FTCM. To change the diameter of the unit cell of FTCM, we changed the dose rate by using a mask aligner (MA6, Karl SÜSS, Germany). The reason is that the area affected by the light diffraction is a function of the dose rate. As shown in Fig. S3, when we changed the dose rate from 150 mJ/cm^2 to 250 mJ/cm^2 incrementally, the unit cell's diameter increased from D = 1.02 μm, 1.28 μm and then to 1.87 μm for the same pitch (3 μm).

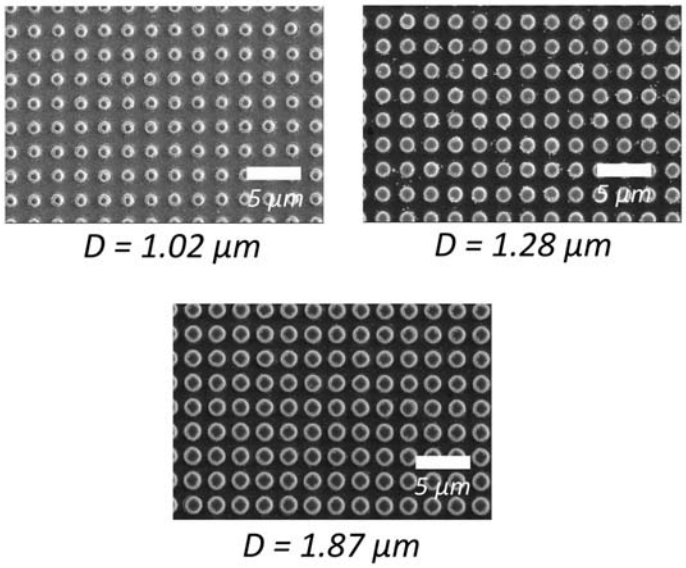

Figure S3. Scanning electron microscope (SEM) images of FTCM structures with diameters (D) = 1.02 μm, 1.28 μm and 1.87 μm for different dose rates, anmely, 150 mJ/cm^2, 200 mJ/cm^2 and 250 mJ/cm^2

4. Effect of imaginary part of refractive index on spectral emissivity of FTCM

In the optics, depending on the wavelength, the material interacts differently with light, since atoms have their intrinsic characteristics such as spring-mass systems[2]. In general, the real part of the refractive index (n) diminishes when increasing the wavelength; this is termed normal dispersion. At a certain wavelength related to the resonance of lattice vibrations, n increases abruptly. Additionally, the imaginary part of refractive index (k) also increases, which induces energy dissipation through the material. This behaviour is termed anomalous (abnormal) dispersion [2]. Silicon nitride shows anomalous dispersion around 8–13 μm which can affect the spectral emissivity of the FTCM. Therefore, we should consider the anomalous dispersion that induces unwanted resonance in the spectrum of interest (8–14 μm).

Figure S4 compares the existence of k for the simulated spectral emissivity with an experimental result. The diameter and pitch of the simulated geometry are 1.87 μm and 3 μm, respectively. As shown in Fig. S4, the simulated emissivity is close to the zero of k. This implies that k has a little impact on the electromagnetic behaviour. Typically, k is related to the absorption coefficient through the material. The absorption coefficient is related to the decay rate of the incident light intensity per unit optical path as follows: $I(x) = I_0 \cdot \exp(-\alpha x)$, $\alpha = 2\omega k/c$ with light intensity I, absorption coefficient α, wave frequency ω and speed of light c. The thickness of silicon nitride in this study was 100 nm, which provided insufficient optical path to affect the spectral emissivity. Additionally, in a metal-dielectric-metal structure, the resistive dissipation in the metal part is the main mechanism of the energy dissipation[3]. Due to the thin layer of dielectric layer, the FTCM also dissipates most of the incident energy through the metal parts. However, we infer that increasing the thickness of dielectric layer can increase the peak around 13.5 μm, because the dissipation through the dielectric layer can affect the spectral emissivity as shown in Fig. S4. Therefore, in the case of the thin dielectric layer shown in Fig. S4, n in the dielectric layer dominated the spectral emissivity of FTCM in this study.

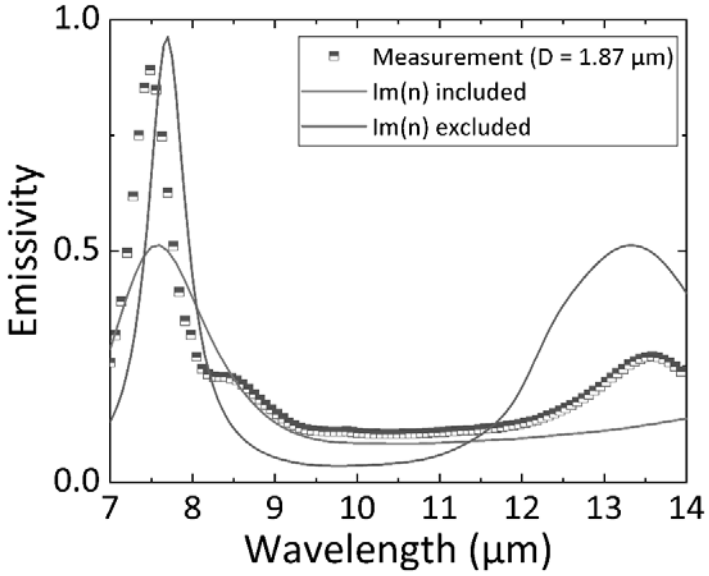

Figure S4. Effect of the imaginary part of the refractive index (*k*) on the spectral emissivity by using simulation.

5. Supersonic flow tunnel for evaluating the IR camouflage performance

In order to check the IR camouflage performance in severe flow conditions, we attach the FTCM on the mock-up airplane in the supersonic flow tunnel. The supersonic flow is one of the extreme conditions with a low temperature (T_{static} ~ 100 K) and high aerodynamic heating ($T_{dynamic}$ ~ 400 K at Mach number = 3, altitude = 10000 m) and high shear force on the surface. We thereby determine that the FTCM have durability. Figure S5 shows schematics of the supersonic flow tunnel facility. Firstly, compressed air is accumulated in the compressed air tank at 15 MPa and the total temperature is 290 K which is controlled by the air conditioning system. After that, by using the pressure regulator, the air pressure is decreased to 0.6 MPa to adjust the mass flow rate in the nozzle neck. Subsequently, in the stagnation chamber, the flow stabilizes to reduce the turbulent intensity through the metal mesh. The compressed air at 0.6 MPa passes through the converging-diverging nozzle and induces Mach number = 3.0 in the test section. In Mach number = 3.0, the static temperature is 104 K with considering the working fluid as an isentropic flow. In the upper part of the test section, the IR window is installed, and we can record the IR image of the specimen part through the window with an IR camera.

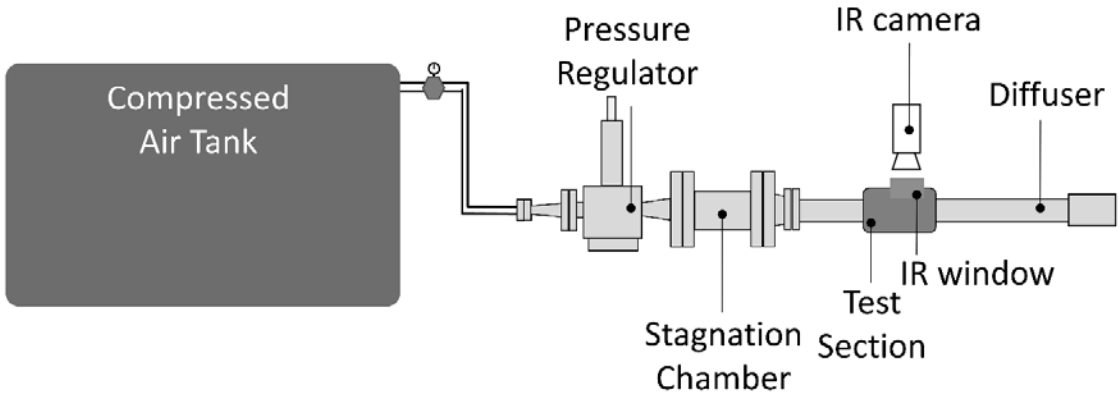

Figure S5. Schematics of the supersonic flow tunnel facility consisting of a tank, a pressure regulator, a stagnation chamber, a converging-diverging nozzle, a test section and a diffuser.

References

(1) M Gere, J. *Mechanics of Materials Sixth Edition*; Copyright, 2004.

(2) Hecht, E. *Optics*; Addison Wesley San Francisco, 2002.

(3) Vora, A.; Gwamuri, J.; Pala, N.; Kulkarni, A.; Pearce, J. M.; Güney, D. Ö. Exchanging Ohmic Losses in Metamaterial Absorbers with Useful Optical Absorption for Photovoltaics. *Sci. Rep.* **2014**, *4*, 4901.

Answers to the 1st Reviewer's Comments

We appreciate the significant efforts that the reviewer put into our paper to review. The reviewer raised comments about the manuscript. We will respond to those suggestions in the following statements. According to the reviewer's opinion, we changed the manuscript with notification by highlighting and attached a full list of changes.

(Comment #1)

The authors have mentioned that the device can be used within 200 °C. What's the limiting operating temperature of the device? Can it tolerate a temperature of 300 °C, 400 °C or 500 °C? Some discussions are recommended.

(Answer)

The polyimide is not endured above 200°C. The reason why we use the polyimide is that the endured temperature is the highest among the flexible substrate in our knowledge. The transition temperature is around 230°C. However, in our study, we target to hide the IR signal caused by the aerodynamics heating against the frontal direction because the IR signal by the aerodynamic heating is significant than we expected [Kim, et al., IEEE Trans. Aerosp. Electron. Syst. 2016, 52]. For this reason, we thought that the polyimide is sufficient to endure the aerodynamic heating in the supersonic fields because the aerodynamics heating can induce up to 180°C at Mach number = 2.0 with the altitude of 5000 m. We add some explanation why we choose the polyimide as a substrate as follow:

Revised and Added Sentences in Introduction (Page. 14)

"…The polyimide typically endures temperatures up to 200°C[42], which indicates that we can utilize the FTCM in the operating condition up to the Mach number = 2.0 at an altitude of 5000 m which is harsh condition of the aircraft. …"

(Comment #2)

What is the temperature for a supersonic flowfield since the camouflage is considered in this scenario?

(Answer)

The reviewer asked about the temperature condition of a supersonic flowfield in our facility. The total temperature of a working fluid consists of two parts such as static temperature and dynamic temperature as following equation: $T_{tot} = T_{stat}$ (Static) + $v^2/2C_p$ (Dynamic) [Ref. Cengel, Y. Heat and mass transfer: fundamentals and applications; McGraw-Hill Higher Education, 2014.]. The measured temperature in the system is the static temperature. In our facility, the total temperature of the working fluid is regulated by 290 K which is controlled by the air conditioning system. In Mach number = 3.0, the static temperature is 104 K based on the assumption of an isentropic flow. We agree with the reviewer's opinion because we omit the temperature value in the supporting information. We, the authors, are thankful for a considerate review and add the temperature value in the manuscript and supporting information as follow:

Revised Sentences in Results 3.3 (Page. 19)

"…The supersonic wind tunnel induced a Mach number = 3.0 with the high shear force. The total temperature of working fluid is 290 K and the static temperature in Mach number 3.0 is 104 K.…"

Revised Sentences in Supporting information (Page. 8)

"…Firstly, compressed air is accumulated in the compressed air tank at 15 MPa and the total temperature is 290 K which is controlled by the air conditioning system.…"

"…In Mach number = 3.0, the static temperature is 104 K with considering the working fluid as an isentropic flow.…"

(Comment #3)
Can the device be fabricated on a large scale? What factors will influence the large-scale fabrication?

(Answer)

In this study, we fabricate FTCM on a 4-inch wafer. Except for the edge of the wafer, the FTCM is fabricated on the substrate successfully. Although the mask aligner provides the possible fabrication of up to a 6-inch wafer, we fail the fabrication of FTCM. We think that there are two needs for a larger-scale fabrication. Firstly, the substrate deposition of polyimide affects the fabrication. In our study, we deposit a liquid polyimide on the substrate with a spin coater. In general, the spin coater makes the flat surface in the center of the substrate, but there are edge beads that induce the non-uniform lithography in the mask aligner. We guess that the increase of spin coating speed can help to increase the fabrication scale. Secondly, the UV uniformity in the mask aligner is an impact on the fabrication. Each UV lamp in the mask aligner has a uniformity range for fabrication. This uniformity affects the size difference along the radial direction. We think that the advanced mask aligner which is better uniform than the present aligner (MA6) can solve this issue for a larger-scale fabrication.

(Comment #4)

This work deals with thermal camouflage with selective energy dissipation, which has also been experimentally demonstrated (Ref.[16] Advanced Functional Materials 2019, 29, 1807319 also deals with MIM structure; Light Science Applications, 2020, 9, 60 and Nature Communications 2021, 12, 18050 demonstrated simultaneous temperature and radiant temperature drop with this strategy).

(Answer)

We, the authors, are thankful for an additional reference. We add the references as follow:

Revised References

(22) Zhu, H.; Li, Q.; Tao, C.; Hong, Y.; Xu, Z.; Shen, W.; Kaur, S.; Ghosh, P.; Qiu, M. Multispectral camouflage for infrared, visible, lasers and microwave with radiative cooling. Nat Commun 2021, 12 (1), 1805. DOI: 10.1038/s41467-021-22051-0. Published Online: Mar. 22, 2021.

(Comment #5)

A scale bar should be added in Figure 4(b) to demonstrate the size of the plane model. For Figure 4(c), there should be a color bar of the infrared temperature.

(Answer)

Based on the reviewer's comment, we revised the figure including the scale and color bar as shown in Fig. 4(b) and (c).

Revised Figure 4 (b) and (c)

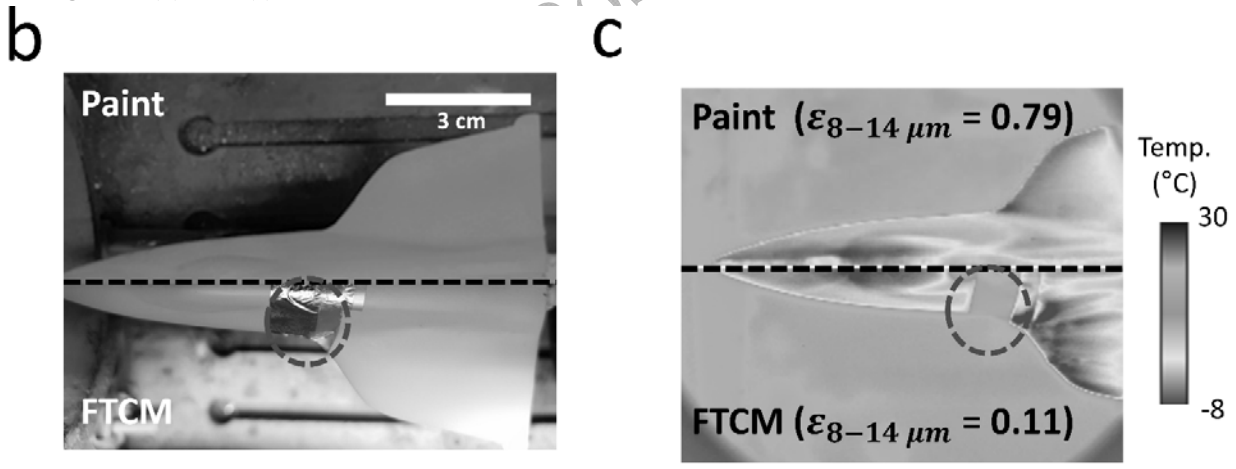

Figure 4. (b) Visible image of the mock-up with various curvatures and wrapped with the FTCMs in the test section. The scale bar represents 3 cm. (c) Comparison of thermographic image of the mock-up in the supersonic flowfield between the gray paint and the FTCMs in the center part. The video clip of thermographic image with FTCMs is provided in the supplementary files.

(Comment #6)

Are they any particular reasons for choosing Au for the metal material and Si3N4 for the space material here?

(Answer)

As mentioned in Comment #6, Al_2O_3 [Dao, T.D., et al., ACS Photon., 2015, 2(7)] and ZnS [Lee, N., et al., ACS Appl. Mater. Interf., 2019, 11(23)] are widely used as a dielectric layer for IR camouflage materials because they are transparent in the IR regime. However, the facility to treat the Al_2O_3 or ZnS around our laboratory is rare, which limits the increase of sample numbers as we want. Typically, silicon oxide (SiO_2) or nitride (Si_3N_4) are widely used as a dielectric layer in micro-nano fabrication. When the thickness of Si is thin enough to realize the transparency in the IR regime, then we think that it is possible to use Si_3N_4 as a dielectric layer.

Figure R1 shows the transmissivity of Si_3N_4 with a thickness of 100 nm in the IR regime. We can understand that there is a small opaqueness from 10 – 14 μm based on the extinction coefficient from the literature [Kischkat, J. et al., Appl. Opt. 2012, 51(28)]. However, we think that the actual extinction coefficient is smaller than the literature because, in our knowledge, the lattice vibration is related to the extinction coefficient which induces the additional resonance in the IR regime [Lee, N., et al., ACS Appl. Mater. Interf., 2020, 12(7)] because there is no additional resonance in the IR regime when using the Si_3N_4. It means that we can use silicon nitride when the thickness is thin enough to ignore the effect of the extinction coefficient.

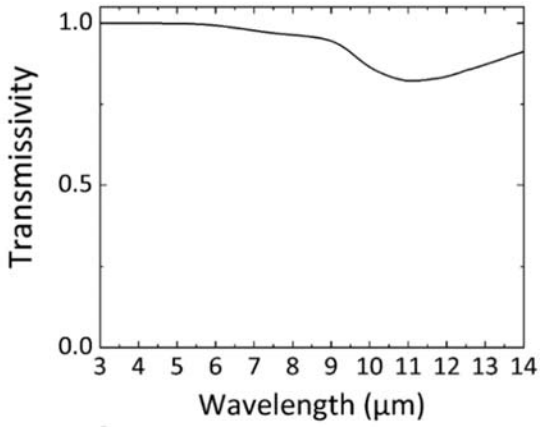

Figure R1. Calculated transmissivity of Si_3N_4 with the thickness of 100 nm used in this study.

Answers to the 2nd Reviewer's Comments

We appreciate the significant efforts that the reviewer put into our paper to review. The reviewer raised comments about the manuscript. We will respond to those suggestions in the following statements. According to the reviewer's opinion, we changed the manuscript with notification by highlighting and attached a full list of changes.

(Comment #1)

The fabricated FTCM was mounted on various non-flat surfaces. The dependence of the simulated spectral emissivity on the diameter and pitch were characterized. The optical properties will also depend on the shape of the pattern. Experiment for different shape will not be needed but some discussion or simulation will be useful to the readers how the shape will change the results.

(Answer)

The reviewer commented that we need to add the discussion of shape effect on the IR spectral emissivity. In general, this study is involved in the frequency selective surface (FSS) [Panwar, R. and Lee, J.R., Aero. Sci. Tech., 2017, 66] because the principle and its performance are the same with FSS regardless of a wavelength [Engheta, N., Science, 2007, 317(5845)]. For FSS surface, several researchers have studied on three types of shape such as symmetric, asymmetric, and double shapes. Firstly, the symmetric shapes such as circle [Kim, et al., Adv. Funct. Mater., 2019, 29(10); Lee, et al., ACS Appl. Mater. Interf., 2020, 12(7)], square [Maier, T. and Brückl, H., Opt. Lett. 2010, 35] and cross [Liu, X., et al., Phys. Rev. Lett. 2011, 107] are widely used because they are independent from the elevation angle and polarization. In addition, the fabrication is easier than other shape types because the size is regular. However, the operating band is narrow which is limited to the broadband operation.

Asymmetric shapes such as bar [Wu, C., et al., Phys. Rev. B, 2011, 84] and c-shape [Liu, B., et al., Nano Lett., 2017, 17] are also used. This asymmetric shape targets the polarization or high independence on the incident elevation than the symmetric shape, which extends its applications to the IR polarizer or filter. However, in case of the IR camouflage material, it is important to be independent from the incident angle without polarization. Therefore, it is not appropriate for the IR camouflage material.

Thirdly, the mixed shape such as concentric shape [Maremi, F., et al., Energies, 11(9); Kim, J., et al., Sci. Rep. 2017, 7] is used for enhancing the bandwidth at the specific wavelength. Since each unit size can be resonant with the target wavelength, the mixed shape increases the number of resonant wavelengths compared to the single shape structure. However, the fabrication is not easy because the different size differs the lithographic time which increases the failure of fabrication based on our experience. Therefore, we choose the circular shape as a unit cell in this study. Based on the reviewer's comments, we also agree to adding the reason of unit cell shape in this study. We add the sentences as follow:

Added Sentences in Results (Page. 9)

"…We choose the circular shape as a unit cell structure in this study. While, in case of asymmetric[36] and mixed shape[37], we can increase the operating band compared to the conventional emitter and the fabrication is easier than the asymmetric shape. Additionally, the circular shape does not induce the polarization and the dependence on the incident angle against the IR detector. For this reason, we judge that the circular shape is appropriate in this study…."

Added References

"(36) Liu, B.; Gong, W.; Yu, B.; Li, P.; Shen, S. Perfect Thermal Emission by Nanoscale Transmission Line Resonators. Nano Lett. 2017, 17 (2), 666–672.
(37) Maremi, F.; Lee, N.; Choi, G.; Kim, T.; Cho, H. Design of Multilayer Ring Emitter Based on Metamaterial for Thermophotovoltaic Applications. Energies 2018, 11 (9), 2299. DOI: 10.3390/en11092299…."

(Comment #2)

The authors discussed "selective emission occurs at 4.9 μm, 6.0 μm and 7.5 μm for diameters of 1.02 μm, 1.28 μm and 1.87 μm, respectively. This implies that the resonant wavelength can be controlled by varying the diameter of a unit cell." Does this mean various diameter features are needed to camouflage for the wide wavelength range?

(Answer)

Ideally, the spectral emissivity in the undetected band is the unity to maximize the energy dissipation due to the IR camouflage in the detected band. However, the selective emitter has an operating limitation because the resonant wavelength is controlled by the metal diameter, which affects the IR camouflage performance [Lee, N., et al., ACS Appl. Mater. Interf., 2019, 11(23)]. In order to overcome this limitation, the mixed diameter can increase the operating band in the undetected band, which helps the energy dissipation against accumulating the infrared signal with decreasing in the detected bands. However, in this study, we concentrate the fabrication of FTCM with disconnecting the brittle part in the MDM structure. For this reason, we show the design point with changing the diameter of unit cell and FTCM operates the same principle of resonant behavior such as the conventional emitter.

(Comment #4)

This device basically looks like a reflector of IR emission from the surrounding. This may mean the device may not camouflage if the IR emission from surrounding is very complex (not a simple uniform just like Figure 1e). Any comment on this issue?

(Answer)

The reviewer asked the issues of the IR reflection from the surrounding. We think that the issue happens at the indoor case. In the room condition, since the distance between the IR detector and target is close, the reflected wave at the specific direction can go into the IR detector directly, which acts like a mirror. This reflected wave sometimes induces the distortion of infrared images as inferred by the reviewer's comment. However, in case of outdoors, the actual signal is different from the indoors. As shown in Fig. R1, this is the example of IR camouflage experiment with a low emissivity material (not FTCM) on the clothes. We understand that a low emissivity material can lower the infrared signal from the surface, which signal is similar to the background. From this result, we recognize that the surrounding has little impact when being close to the actual case.

Figure R2. Infrared images on the clothes depending on the attachment of low emissivity material

(Comment #5)

Dependence of the measured spectral emissivity of the FTCM on the incident angle was provided in Figure 3a. It looks like there is considerable angle dependence on the emissivity. And this may make some problems on the camouflage for a highly non-flat surface where the incident angles will vary a lot depending on the spots as the authors mentioned that This result is important since the detector can seek the target by varying the incident angle. Any solution for this issue?

(Answer)

In Fig. 3(a), we suggested the measured spectral emissivity on the incident angle. In our opinion, there are two reasons which are not crucial impact on the IR camouflage performance. Firstly, the independence of selective emission is up to 60°, which value is large enough to cover the target. If the target is the leading edge of the aircraft, then we can only recognize 1/3 part of the whole leading-edge part. In case of the recognition of IR camouflage, the difference of IR signal between target and background, and chasing time of predator are important [Kim, et al., IEEE Trans. Aerosp. Electron. Syst. 2016, 52]. Based on this reference, we recognize that a decrease of IR signal by 60% from the target makes twice larger survivability of the target. Thus, we think that the independence of spectral emissivity in FTCM is sufficient. Secondly, we recognize the IR camouflage performance on the high arbitrary surface in Fig. 1(e) and Fig. 4(c) as follow:

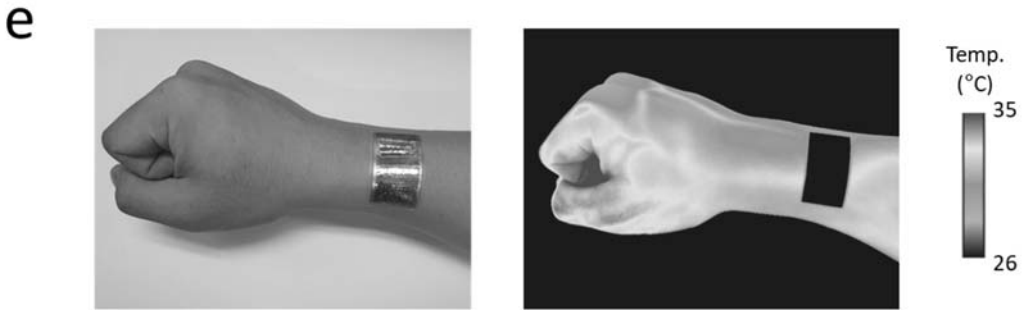

Figure 1(e) Qualitative evaluation of the IR camouflage performance of the FTCM (left: visible image; right: thermographic image (8-14 μm).

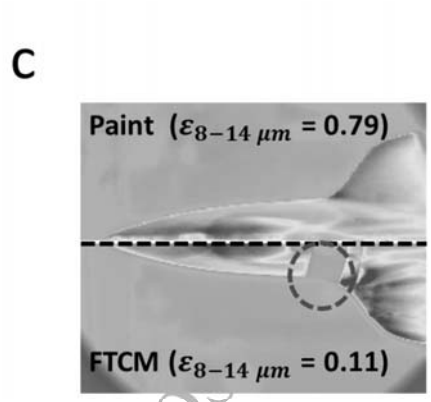

Figure 4(c) Comparison of thermographic image of the mock-up in the supersonic flowfield between the gray paint and the FTCMs in the center part. The video clip of thermographic image with FTCMs is provided in the supplementary files.

In figures, although the incident angle is large at the arm or the edge of aircraft, the IR camouflage happens. It means that the IR camouflage performance maintain despite to the loss of selective emission. Although the decrease of selective emission decreases the energy dissipation, this value is smaller than expected because the integration of elevation angle of emissive energy is proportional to the trigonometric functions.

(Comment #6)

The camouflage in wideband spectrum range shows a wider application field. Even though the authors focused on the IR range, there are other recent researches on broadband wearable camouflage such as visible to IR range camouflage (Adv. Funct. Mater., 30, 2003328 (2020)). Those recent progress needs to be discussed along with other attempts for IR camouflage studies.

(Answer)

We are thankful for your considerate comments. We also agree to the reviewer's opinion because the thermoelectric materials are one of the ways to realize the IR camouflage in the actual field. We added the additional reference related to the IR camouflage material as follow:

Added References

"(15) Lee, J.; Sul, H.; Jung, Y.; Kim, H.; Han, S.; Choi, J.; Shin, J.; Kim, D.; Jung, J.; Hong, S.; Ko, S. H. Thermally Controlled, Active Imperceptible Artificial Skin in Visible-to-Infrared Range. Adv. Funct. Mater. 2020, 30 (36), 2003328. DOI: 10.1002/adfm.202003328."

(Comment #7)

In the spectral emissivity of the FTCM in the range 3–14 μm (Figure 2(a)), For the FT-IR measurement, I wonder whether the integrating sphere was used.

(Answer)

The reviewer asked the use of integrating sphere for evaluating the spectral emissivity. We use the spectral directional emissivity in this study exactly. As mentioned by the reviewer's comments, if we want to express the emissivity, it is needed to integrate the emissive energy along the whole sphere. However, by using the FT-IR measurement, it is impossible to integrate the whole energy along the azimuthal and elevation angle because the elevation angle is limited from 13 – 85° and the reflected signal is distorted above 75° from the front direction because every surface cannot be diffuse surface. However, since many researchers in the IR camouflage have also understood this limitation of emissivity measurement, we measure the spectral directional emissivity.

(Comment #8)

For the practical application, the fabricated FTCM layer will be mounted on the outermost surface of the target application and it should have enough mechanical stability against the mechanical perturbation such as rubbing, scratching etc. At this stage, the reliability issue may not be considered seriously. Some discussion on this reliability issue needs to be provided.

(Answer)

We also agreed to the reviewer's opinion because the reliability issue is weak point in the micro-nano structure. For this reason, we develop the method for increasing the reliability of micro-nano structure. However, since we do not discuss the reviewer's opinion in the manuscript, we add the sentences in the conclusion as follow:

Added Sentences in Conclusion (Page. 21)

"...Although, in order to utilize this material for the actual applications, the mechanical reliability should be secured against the mechanical perturbation such as rubbing and scratching, we hope that the FTCM show a way to develop flexible materials with brittle materials for radiative cooling, energy conversion, and space applications. In addition,

the current limitations can be overcome by the additional structure to protect the micro-nano structure which is fragile against the external perturbation.…"

Answers to the 3rd Reviewer's Comments

We appreciate the significant efforts that the reviewer put into our paper to review. The reviewer raised comments about the manuscript. We will respond to those suggestions in the following statements. According to the reviewer's opinion, we changed the manuscript with notification by highlighting and attached a full list of changes.

(Comment #1)

In previously published papers by other authors, such as Adv. Optical Mater. 2018, 1801006, the flexible spectrally selective infrared stealth materials has been demonstrated. Why do anthors say "However, flexible camouflage materials are still unsolved" in the abstract? What is the difference between this work and the previous work in the flexibility?

(Answer)

The reviewer asked the difference between this work and the precious work in the flexibility. We agreed to the reviewer's opinion because the flexibility itself is not unsolved issues in the field. We already knew that there are several studies about the material flexibility with IR camouflage in this field. Our intention of this sentence is to maintain the IR spectral emissivity compared to the conventional IR emitter. In our previous work [Ref. Adv. Func. Mater. 2018, 29(10)], we already tried to make a flexible material in the IR regime. We transferred the flexible IR camouflage materials from a substrate (Si) to a target surface, then we measured the IR emissivity. The MDM structure consisted of Au (200 nm) – ZnS (200 nm) – Au (200 nm). We measured that the flexible material has lower performance compared to the conventional emitter and the small particles existed on the MDM structure. We thought that this is related to the failure of the dielectric material in the structure.

As we know, the dielectric material is very fragile with external stress [Ref. Luo, J, et al., Nano Lett. 2016, 16(1), 105–113]. In the reference, the elongation below 0.1% of the total characteristic length can break the brittle material despite to the small scale of material (O~20 nm). This can be applied to the MDM structure because the dielectric material (200 nm) is much thicker than the reference. Also, it is possible to apply for the brittle material such as semiconductor (Si, Ge, etc) and dielectric (ZnS, SiO_2, Si_3N_4, etc) materials. Therefore, we try to disconnect the dielectric material to reduce the mechanical stress.

Considering the reviewer's opinion, we revise the abstract and add some references related to the flexibility of IR camouflage material as follow:

Revised Abstract (Page. 2)

"…However, flexible camouflage materials are still challenging issues because of the material's brittleness and anomalous dispersion….."

Added the sentences in Introduction (Page. 4)

"…Some of research have suggested the flexible structure with thin films in the brittle part[22,32], however, their thicknesses are still thicker than the free of fracture[31]…."

Added the references

(15) Lee, J.; Sul, H.; Jung, Y.; Kim, H.; Han, S.; Choi, J.; Shin, J.; Kim, D.; Jung, J.; Hong, S.; Ko, S. H. Thermally Controlled, Active Imperceptible Artificial Skin in Visible-to-Infrared Range. Adv. Funct. Mater. 2020, 30 (36), 2003328. DOI: 10.1002/adfm.202003328.

(21) Zhu, H.; Li, Q.; Zheng, C.; Hong, Y.; Xu, Z.; Wang, H.; Shen, W.; Kaur, S.; Ghosh, P.; Qiu, M. High-temperature infrared camouflage with efficient thermal management. Light Sci. Appl. 2020, 9, 60. DOI: 10.1038/s41377-020-0300-5.

(22) Zhu, H.; Li, Q.; Tao, C.; Hong, Y.; Xu, Z.; Shen, W.; Kaur, S.; Ghosh, P.; Qiu, M. Multispectral camouflage for infrared, visible, lasers and microwave with radiative cooling. Nat. Commun. 2021, 12(1), 1805. DOI: 10.1038/s41467-021-22051-0. Published Online: Mar. 22, 2021.

(32) Peng, L.; Liu, D.; Cheng, H.; Zhou, S.; Zu, M. A Multilayer Film Based Selective Thermal Emitter for Infrared Stealth Technology. Advanced Optical Materials 2018, 6 (23), 1801006. DOI: 10.1002/adom.201801006…."

(Comment #2)

In the introduction, the review of present research about the spectrally selective infrared stealth materials is not comprehensive. For example, as a different and effective way, recent work about spectrally selective infrared stealth materials based on ultrathin Ag/Ge (Adv. Optical Mater. 2018, 1801006) should be cited.

(Answer)

The reviewer commented that we, the authors, should add more references related to the IR camouflage materials in this file. We agree to the reviewer's opinion, because it is our mistake to omit some references in this field. Therefore, we add some references as follow. We are thankful for the reviewer's considerate comments to improve the article quality.

Added the references

(32) Peng, L.; Liu, D.; Cheng, H.; Zhou, S.; Zu, M. A Multilayer Film Based Selective Thermal Emitter for Infrared Stealth Technology. Advanced Optical Materials 2018, 6 (23), 1801006. DOI: 10.1002/adom.201801006…."

(Comment #3)

What is the waveband emissivity of the FTCM in the 3-5 μm, 5-8 μm and 8-14 μm, respectively? Authors should provide the accurate values.

(Answer)

The reviewer commented that we need to suggest the quantitative emissivity in the 3-5 μm, 5-8 μm and 8-14 μm. We agree to the reviewer's comment because the value of radiative energy can make a confusion for a general reader. We suggested the radiative energy in undetected and detected bands because some of readers are not familiar to the surface emissivity compared to the energy. However, as the reviewer's comments, we should provide the quantitative value to express how much the emissivity is changed due to the FTCM.

The emissivity of FTCM in 3-5 μm, 5-8 μm and 8-14 μm is 0.12, 0.27 and 0.16, respectively. This value is not ideally spectral emissivity for IR camouflage performance which value is 0, 1 and 0 in 3-5 μm, 5-8 μm and 8-14 μm, respectively. Compared to the convectional IR camouflage material ($\varepsilon_{3\text{-}5\ \mu m} = 0.15$, $\varepsilon_{5\text{-}8\ \mu m} = 0.42$, $\varepsilon_{8\text{-}14\ \mu m} = 0.11$), the emissivity value is similar to the FTCM. It means that the IR camouflage performance of FTCM is identical with the conventional IR camouflage material despite having a material flexibility. Based on the reviewer's comments, we add the value of emissivity in FTCM and conventional emitter as follow:

Added the sentences in Results (Page. 15)

"...It means that the wideband emissivity in 3–5 μm and 8–14 μm are 0.12 and 0.16, respectively. These values are similar to the conventional emitter which are 15% and 11% of blackbody's radiative energy in the ranges of 3–5 μm ($\varepsilon_{3\text{-}5\ \mu m} = 0.15$) and 8–14 μm ($\varepsilon_{8\text{-}14\ \mu m} = 0.11$), respectively. At the same condition, the metal surface shows radiative energies that 9% and 8% of blackbody's radiative energy in the ranges of 3–5 μm ($\varepsilon_{3\text{-}5\ \mu m} = 0.09$) and 8–14 μm ($\varepsilon_{8\text{-}14\ \mu m} = 0.08$), respectively. ..."

"... In the case of the FTCM, the dissipative energy and wideband emissivity in the undetected band is 63.1 W/m^2 and 0.27, which is 2580% greater than that of the metal surface. Even though conventional metamaterials (98.7 W/m^2 and 0.42) show 36% higher energy dissipation compared with the FTCM, we think that the FTCM have camouflage performance comparable to that of a conventional camouflage surface because of its flexibility and machinability. ..."

(Comment #4)

Authors should compare the infrared stealth performances between the FTCM and common low emissivity infrared stealth materials in the supersonic flowfields through infrared images.

(Answer)

The reviewer recommended that we, the authors, try to measure the additional infrared images of common low emissivity infrared stealth materials in the supersonic flowfield. Unfortunately, it is difficult to perform the experiment with common stealth materials in the supersonic flowfield. In the supersonic flowfield, there are large shear stress on the surface which induces large momentum and lift force on the specimen. It means that we need to attach the specimen on the surface tightly. However, on the one hand, some of IR camouflage materials such as conventional emitters, ITO or metal plate are brittle which cannot attach the arbitrary surface in the supersonic flowfields. They detach from the surface and induce safety issues in the supersonic flowfield. On the other hand, the deposition of Au or Ag is not easy on the arbitrary surface in Fig. 4(c).

However, we, the authors, agree to the reviewer's opinion partially, because it is needed to show the comparions of IR camouflage performance in the supersonic flowfield directly. For this reason, we compare the IR images between the paint (MIL-PRF-85285) and paint with FTCM at the same angle. In case of the paint, it is widely used for the aircraft. We are thankful for the reviewer's comment and revise the figure and caption as follow:

Added and revised the sentences in Results (Page. 15)

"...Figure 4(b) shows the mock-up of the target surface covered with the military paint (MIL-PRF-85285) and wrapped with the FTCM. ..."

"...Figure 4(c) shows the comparison of IR images between the mock-up wrapped with and without the FTCM. In Fig. 4(c), the wrapped part is assimilated with the environment and hides its IR signature against the IR detector. In the case of the bare surface coated with paint, the IR signature is different from the background, which leads to the higher susceptibility of the target against the IR detector...."

Revised Figure 4

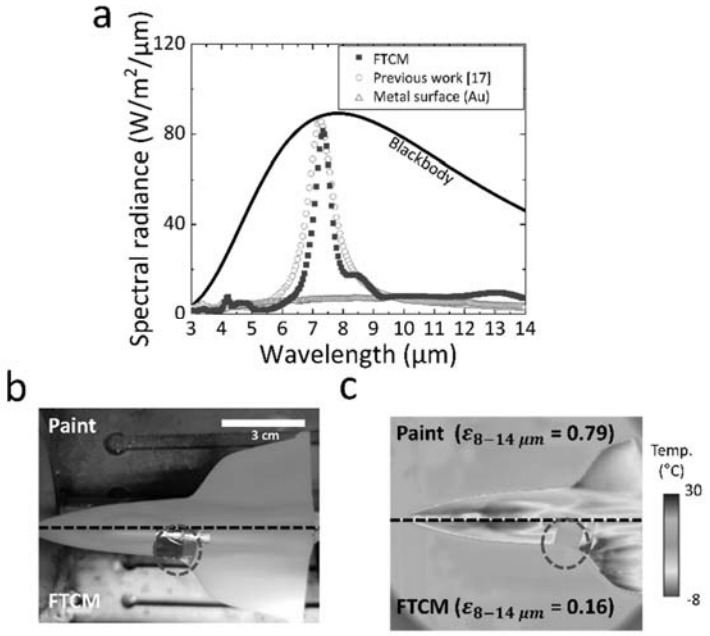

Figure 4. (a) Spectral radiance of the FTCM, conventional IR camouflage materials and blackbody. (b) Visible image of the mock-up with various curvatures and wrapped with the FTCMs in the test section. The scale bar represents 3 cm. (c) Comparison of thermographic image of the mock-up in the supersonic flowfield between the gray paint and the FTCMs in the center part. The video clip of thermographic image with FTCMs is provided in the supplementary files.

(Comment #5) The preparation process in the manuscript is extremely complicated. To prepare the FTCM, the author has successively used various processes such as spin coating, electron beam evaporation, and plasma enhanced chemical vapor deposition. In addition, photolithography is also a necessary factor to achieve surface microstructure. These processes are costly and time-consuming, which is not conducive to the application of materials in actual engineering.
(Comment #6) Although the problem of flexible materials is overcome, the process used in the manuscript is difficult to prepare on a large area. For weapons and equipment such as aircraft, the surface size is usually very large. It is very difficult to completely cover it with FTCM. The prospects for the actual use of the FTCM are questionable.

(Answer)

The reviewer commented that the FTCM is too expensive and not practical for the actual application. We agreed to the reviewer's opinion partially because, in order to approach the ideal performance of IR camouflage performance, we did not consider the cost and practical consideration in this study. In addition, every researcher has a question because the final goal of this study utilizes FTCM for the real application as mentioned in the comment. However, we think that this study makes a stepping-stone on the possibility of flexible material for IR camouflage and proves similar performance to the conventional IR camouflage material.

As mentioned above the answer in the Comment #1, the brittle material for IR camouflage material has a problem because it can lower performance or unsuitable for arbitrary surfaces. By changing the strategy such as

disconnecting the brittle part of conventional IR emitter, we realize FTCM having a material flexibility as well as high IR camouflage performance. In addition, we prove the FTCM enduring the supersonic flow field which induces the high shear stress and extreme temperature condition on the surface. They express that the IR camouflage material based on FTCM can be operated in the supersonic flowfield with IR camouflage performance on an arbitrary surface.

Moreover, we also need to mention the complexity and cost of IR camouflage material. Many studies related to IR camouflage material such as thermoelectric materials [Ref. Lee, J, et al., Adv. Funct. Mater., 2020, 30(36); Hong, S, et al., Adv. Funct. Mater., 2020, 30(11)] or thin film [Ref. Zhu, H., et al., Light, Sci. Appl. 2020, 9, 60; Kim, T., et al., Adv. Funct. Mater. 2019, 29(10); Salihoglu, O., et al., Nano Lett. 2018, 18(7); Peng, L., et al., Adv. Opt. Mater. 2018, 6(23);] have their weaknesses because of complicated fabrication, need of additional power supply, cost of material and others. In this study, our weakness is the reviewer's comments such as complex fabrication and cost of material. However, in the state of the art of micro-nano fabrication, every IR camouflage material cannot be applied to the practical applications because the cost is too expensive, and the fabrication is too complex to cover the whole parts. For this reason, we understand that every IR camouflage material suggest a stepping-stone for the actual applications.

In our knowledge, in order to realize this material for the practical application, we need to have several steps as follow. Firstly, we change the material from Au or Ag to Cu or Al. In the IR regime, the polished metal acts as a perfect conductor. We can infer that the common metal can be used as a metal part in a metal-dielectric-metal structure. Secondly, we think that the advanced transfer-engineering of micro-nano structure with the imprint lithography [Ref. Kang, S-I., Micro/Nano replication: processes and applications, Wiley; Lee, C.H. et al., ACS Nano, 2014, 8, 8746] is needed. The nanoimprint technology is one of key technologies because it can relate to the mass production process. The speed and size of a fabrication are up to 30 m/min with the width of 250 mm [Ref. Leitgeb, M., et al., ACS Nano, 2016, 10] in the current technology. If this fabrication speed is up to 100 m/min with the width of 1 m, then we can imagine the mass production of FTCM being possible for the practical application. Thirdly, we need to develop the paint-like IR camouflage material. Even though the roll-to-roll technology is powerful, the best option is a paint-like material. Several studies already suggested the low emissivity paint which is mixed with the military paint and metal powders [Ref. Wang, L., et al., Surf. Coat. Tech. 2019, 357, 559-566]. However, the mixed paint just lowers the overall emissivity which can induce the thermal instability as mentioned in the manuscript. If functional particles which interacts with the electromagnetic wave in the paint will be developed, this is also one of the options to achieve the practical IR camouflage material.

(Comment #7)

The language should be improved.

(Answer)

The reviewer asked us to improve the language in the manuscript. We already performed the professional editing service and attached the certificate as follow.

EDITORIAL CERTIFICATE

Date: June 22, 2021

Manuscript Author(s): Hyung Hee Cho

Manuscript Title: Flexible Thermo-Camouflage materials in Supersonic Flowfields with Selective Energy Dissipation

To Whom It May Concern:

This letter confirms that the manuscript corresponding to the information detailed above was edited by a professional, native English-speaking editor at Wordvice.

We guarantee 100% language accuracy in the text, as edited and delivered to the author(s) on the date below. We make no claims as to the substantive matter covered by the paper and have not altered the intent or research content drafted by the author(s).

The author(s) may accept or reject any of our comments or suggestions upon receipt of the document we edited. Should you have any questions or concerns, please contact Wordvice at edit@wordvice.com

Sincerely,
Wordvice

Wordvice is a premier international English editing service. Our mission is to help researchers, scholars, students, and professionals reach their full potential through clear communication in their writing. By providing premium English editing services at affordable rates to clients from around the world, Wordvice seeks to tear down language barriers and contribute to the advancement of research and education.

Signature

Kevin Heintz
Managing Editor, Wordvice

Date of Issue

July 22, 2021

Contact Wordvice

KOREA | U.S. | JAPAN | TAIWAN | CHINA | TURKEY

Figure R3. Certificate of professional English editing service for this manuscript

Answers to the 3rd Reviewer's Comments

We appreciate the significant efforts that the reviewer put into our paper to review. The reviewer raised comments about the manuscript. We will respond to those suggestions in the following statements. According to the reviewer's opinion, we changed the manuscript with notification by highlighting and attached a full list of changes.

(Comment #1)

In the abstract "we quantified the IR camouflage performance of FTCM that energy dissipation of a metal surface (Au) by 2580% in the undetected band (5–8 μm), and the IR signature of blackbody by 12% (3–5 μm) and by 16% (8–14 μm) in the detected bands.", why is the energy in the non-detection band compared to metal, and the energy in the detection band is compared to blackbody, but not the other way around. We believe that the energy of the non-detection band should be compared with the black body, so that its heat dissipation performance can be measured. The energy of the detection band should be compared with that of metal, highlighting its low emissivity performance. The author should not confuse the reader in order to show that his results are good. Authors should quantitatively use emissivity values to express performance, not percentages. This must be changed.

(Answer)

As the reviewer mentioned, we agree that it is possible to make a confusion for understanding of the essential message in this article. For this reason, we revise the manuscript as suggested by the reviewer.

Revised Abstract (Page. 2)

"…We quantified the IR camouflage performance of FTCM that the emissivity in the undetected band (5–8 μm) is 0.27, and the emissivity in detected bands are 0.12 (3–5 μm) and 0.16 (8–14 μm) in the detected bands, respectively. …"

(Comment #2)

Authors should compare the infrared stealth performances between the FTCM and common low emissivity infrared stealth materials. If there is difficulty in in the supersonic flowfields, it should be performed in the commom environment. In the revised paper, authors compare the infrared stealth performances between the FTCM and MIL-PRF-85285. But what is the emissivity curve of the military paint (MIL-PRF-85285). The emissivity is high in 3-14 μm, so this reference sample is not proper. The common low emissivity infrared stealth materials should be selected. The sample should have similar emissivity with FTCM in the 3-5 and 8-14 μm and different emissivity in the 5-8 μm. Otherwise, it can't prove that FTCM has excellent performance, so it's better not to do it.

(Answer)

The reviewer suggested that we, the authors, need to compare IR images such as low emissivity materials and FTCM. For this reason, we compare the spectral emissivity and IR images on the heated plate which temperature is 370 K of the total temperature of Mach number = 1.5 at 5000 m. The added sentences and figure are shown as follow:

Revised Figure

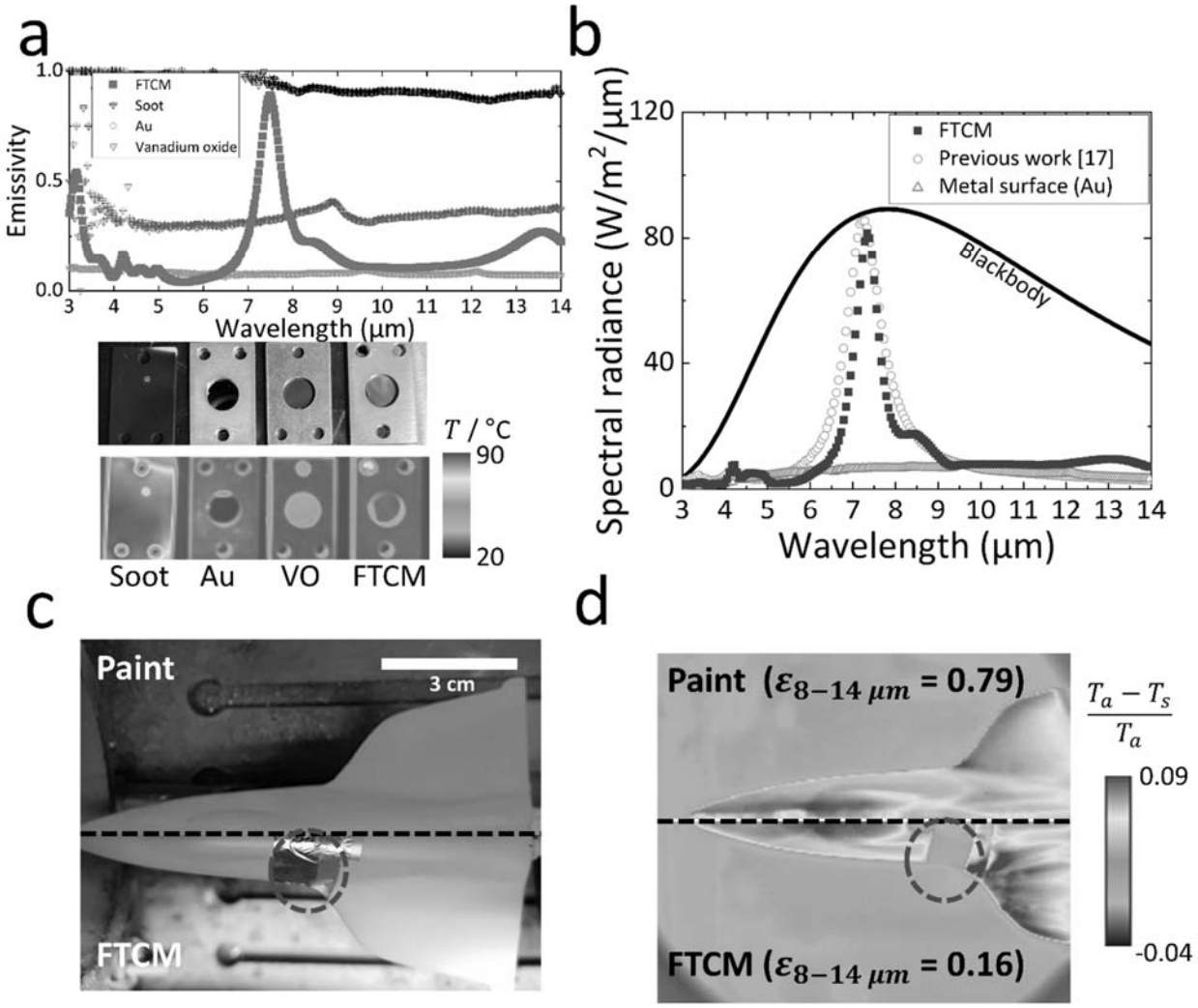

Figure 4. (a) Spectral emissivity and IR images of several surfaces such as Au, FTCM, Soot and Vanadium oxide (VO). The heated surface temperature is 370 K which is controlled by the heating plate. (b) Spectral radiance of the FTCM, conventional IR camouflage materials and blackbody. (c) Visible image of the mock-up with various curvatures and wrapped with the FTCMs in the test section. The scale bar represents 3 cm. (d) Comparison of thermographic image of the mock-up in the supersonic flowfield between the gray paint and the FTCMs in the center part. T_s and T_a are the surface temperature and the ambient temperature, respectively. T_a is 290 K controlled by the air-conditioning system. The video clip of thermographic image with FTCMs is provided in the supplementary files.

Added and Revised Sentences (Page. 18-19)

"...Firstly, we compare IR images such as Au, Soot, Vanadium oxide (VO) and FTCM. The measured spectral emissivity is presented in Fig. 4(a). Au and Soot surface presents the lowest and highest emissivity in infrared regime (3-14 μm), respectively. Vanadium oxide is a reference surface which is used for the radiation control surface[43], which value is 0.4 in infrared regime. The IR image in 8-14 μm shows that the apparent temperature of FTCM is close to the Au surface compared to VO. It means that FTCM is higher camouflage performance than VO.

Secondly, by assuming diffusive emission from the surface, we can evaluate the spectral irradiance of a blackbody using following equation[14]:…"

Added the references

"(43) Kats, M. A.; Blanchard, R.; Zhang, S.; Genevet, P.; Ko, C.; Ramanathan, S.; Capasso, F. Vanadium Dioxide as a Natural Disordered Metamaterial: Perfect Thermal Emission and Large Broadband Negative Differential Thermal Emittance. Phys. Rev. X 2013, 3 (4), 041004."

(Comment #3)

For citations and references, papers should be objective, comprehensive, and fair to ensure that readers have a comprehensive and accurate understanding of relevant background information, and scientificity should be pursued. In the sentences "Several researchers have developed IR camouflage materials satisfying these requirements and demonstrated IR camouflage performance by using an IR camera18,20,25" and "In case of the emissivity-controlled materials, they do not need no additional devices and larger controlling range of IR signature17–22", the recent work about spectrally selective infrared stealth materials based on ultrathin Ag/Ge (Adv. Optical Mater. 2018, 1801006) should be cited and added in the above places. This document proposes a new spectrally selective infrared stealth material that can be prepared on a large area, and as far as I know it is the earliest that thermal images were taken with an infrared thermal imager, and compared it to the common low emissivity materials to prove the superiority of spectrally selective radiator for infrared stealth. So, from an objective point of view, I think it needs to be added.

(Answer)

The reviewer commented that we need to change the reference at the specific location in the manuscript. We agreed to the reviewer's opinion and changed the location in the manuscript as follow:

Added the references

(23) Peng, L.; Liu, D.; Cheng, H.; Zhou, S.; Zu, M. A Multilayer Film Based Selective Thermal Emitter for Infrared Stealth Technology. Advanced Optical Materials 2018, 6 (23), 1801006. DOI: 10.1002/adom.201801006…."